COHERENT ANTI-STOKES RAMAN SPECTROSCOPY USING TUNABLE DYE LASERS PUMPED BY AN ULTRAVIOLET NITROGEN LASER

Richard Wayne Gilbert

THESIS

COHERENT ANTI-STOKES RAMAN SPECTROSCOPY USING TUNABLE DYE LASERS PUMPED BY AN ULTRAVIOLET NITROGEN LASER

by

Richard Wayne Gilbert

June 1975

Thesis Advisor: W. M. Tolles

UNCLASSIFIED

SECURITY CLASSIFICATION OF THIS PAGE (When Data Entered)

REPORT DOCUMENTATION PAGE		READ INSTRUCTIONS BEFORE COMPLETING FORM
1. REPORT NUMBER	2. GOVT ACCESSION NO.	3. RECIPIENT'S CATALOG NUMBER
4. TITLE (and Subtitle) Coherent Anti-Stokes Raman Spectroscopy Using Tunable Dye Lasers Pumped by an Ultraviolet Nitrogen Laser		5. TYPE OF REPORT & PERIOD COVERED Master's Thesis; June 1975 6. PERFORMING ORG. REPORT NUMBER
7. AUTHOR(s) Richard Wayne Gilbert		8. CONTRACT OR GRANT NUMBER(s)
9. PERFORMING ORGANIZATION NAME AND ADDRESS Naval Postgraduate School Monterey, California 93940		10. PROGRAM ELEMENT, PROJECT, TASK AREA & WORK UNIT NUMBERS
11. CONTROLLING OFFICE NAME AND ADDRESS Naval Postgraduate School Monterey, California 93940		12. REPORT DATE June 1975 13. NUMBER OF PAGES 135
14. MONITORING AGENCY NAME & ADDRESS(if different from Controlling Office)		15. SECURITY CLASS. (of this report) Unclassified 15a. DECLASSIFICATION/DOWNGRADING SCHEDULE
16. DISTRIBUTION STATEMENT (of this Report) Approved for public release; distribution unlimited.		
17. DISTRIBUTION STATEMENT (of the abstract entered in Block 20, if different from Report)		
18. SUPPLEMENTARY NOTES		
19. KEY WORDS (Continue on reverse side if necessary and identify by block number) Raman Spectroscopy Nitrogen Laser Dye Laser CARS		

20. ABSTRACT (Continue on reverse side if necessary and identify by block number)

An apparatus to observe the nonlinear generation of coherent anti-Stokes Raman beams was constructed. Three different types of nitrogen lasers were built and each was critically evaluated. One type, which provided the highest

DD FORM 1 JAN 73 1473 (Page 1)

EDITION OF 1 NOV 68 IS OBSOLETE

S/N 0102-014-6601

UNCLASSIFIED

SECURITY CLASSIFICATION OF THIS PAGE (When Data Entered)

(20. ABSTRACT Continued)

power, was used to simultaneously pump two tunable dye lasers. The backgrounds and design features of each of the laser types are discussed. When two dye laser beams were crossed and focused in a Raman active material, the sample emitted higher frequency anti-Stokes radiation. Due to system limitations, this radiation was diffuse rather than a collimated beam. The theory of Coherent Anti-Stokes Raman Spectroscopy (CARS) is also discussed.

Coherent Anti-Stokes Raman Spectroscopy Using Tunable Dye Lasers Pumped by an Ultraviolet Nitrogen Laser

by

Richard Wayne Gilbert
Lieutenant, United States Navy
B.S., University of California, Davis, 1968

Submitted in partial fulfillment of the
requirements for the degree of

MASTER OF SCIENCE IN PHYSICS

from the

NAVAL POSTGRADUATE SCHOOL
June 1975

ABSTRACT

An apparatus to observe the nonlinear generation of coherent anti-Stokes Raman beams was constructed. Three different types of nitrogen lasers were built and each was critically evaluated. One type, which provided the highest power, was used to simultaneously pump two tunable dye lasers. The backgrounds and design features of each of the laser types are discussed. When two dye laser beams were crossed and focused in a Raman active material, the sample emitted higher frequency anti-Stokes radiation. Due to system limitations, this radiation was diffuse rather than a collimated beam. The theory of Coherent Anti-Stokes Raman Spectroscopy (CARS) is also discussed.

TABLE OF CONTENTS

LIST OF TABLES

LIST OF ILLUSTRATIONS

ACKNOWLEDGMENT

The author wishes to thank Dr. W. M. Tolles for accepting this project and for spending many long hours digesting the reams of material involved in preparing for it. Many of the concepts and designs were foreign to everyone concerned and a great deal of time was involved in the analysis of available systems and in the construction of the lasers. R. Sanders also deserves special recognition for his invaluable assistance in the construction and troubleshooting of the apparatus.

Special appreciation goes to my wife, Nancy, for understanding the long hours of isolation and for providing constant encouragement during the rough times.

I. INTRODUCTION

Coherent Anti-Stokes Raman Spectroscopy (CARS) is a recently developed method that shows great promise for extending and complementing the applicability of standard Raman spectroscopic techniques. The Raman effect, recognized since 1928, is a very useful method for observing molecular vibrational energy differences but the conversion efficiency is low, the output signal is sometimes weak and the signal to noise ratio is often unacceptable. The introduction of the laser made it possible to use smaller samples and simultaneously observe more intense outputs. The detection of the signal against the background fluorescence continued to be a serious problem, however. Coherent anti-Stokes emission seems to overcome many of these shortcomings. CARS provides a tremendous increase in the conversion efficiency, occurs at a shorter wavelength than natural fluorescence, utilizes relatively moderate input powers and, because of its coherent nature, facilitates signal separation.

Since both the real and imaginary parts of the polarizability are involved, the coherent anti-Stokes Raman effect has also been variously reported as four wave mixing and three-photon absorption. In this effect, two laser beams are focused together in the sample to be analyzed. When the frequency (photon energy) difference of the two lasers

equals the sample's vibrational energy difference, a third laser beam at the anti-Stokes frequency emerges. To satisfy the phase matching requirement, the anti-Stokes beam emerges at an angle slightly off that of the entering beams. This enables the use of spatial filters to isolate the beam of interest.

Tunable dye lasers have proved to be an ideal source of radiation for this form of Raman study. The dye laser has a large characteristic gain resulting in high peak powers and an emission profile covering a wide range of wavelengths. Of the many methods available for pumping dye lasers, the nitrogen laser is often chosen. The molecular nitrogen laser is comparatively inexpensive and easy to construct and produces high peak-power pulses.

The final objective of the study presented in this paper is the observation of the coherent anti-Stokes radiation caused by the mixing of the two laser beams. To this end, however, various modifications and trade-offs had to be made during the construction of the nitrogen and dye lasers and these are, therefore, considered an integral part of the report. Section II deals with the dye laser pump. It includes a discussion of the various types of pumps currently being used with dye lasers and the features of each. The nitrogen laser is then presented theoretically and practically. During the course of the experimental work, three different types of nitrogen lasers were

constructed and operated. These are evaluated with respect to output power, pulsewidth and efficiency.

The dye lasers themselves are discussed in Section III. Two tunable dye laser cavities are needed for this work. One is a reasonably low power, fully tunable source to produce the Stokes frequency light. The other is a fixed-frequency, high power pump source. In order to keep the pump radiation approximately constant during mixing, it should be at least several times as powerful as the Stokes beam. In Section III, the various types of dye laser models, tuning elements and procedures are reviewed. The actual construction and operation of the dye lasers used are discussed and compared to theory and current literature.

Section IV starts with a presentation of the theory of Raman Spectroscopy in general and Coherent anti-Stokes Raman Spectroscopy in particular. The background is briefly reviewed and the theoretical aspect is developed in depth. Of primary importance is the amplification of the non-linear susceptibility equations and their relation to the current investigation. In the final analysis, the efficiency of the anti-Stokes output is proportional to the square of the non-linear susceptibility and the square of the pump intensity. It then becomes obvious that a strong pump beam, along with the Stokes beam, must be tightly focused in the sample. Section IV continues with the actual experimental apparatus used and the results obtained. The anti-Stokes output fully

demonstrates the feasibility of this method for the observation of the vibrational characteristics of molecules. With additional work, including stabilization of the laser intensities, this method could become important in future applications such as sample identification and monitoring.

II. THE DYE LASER PUMP

There are a great number of optical pumps which can be used to stimulate a dye laser. Power, cost and size requirements are usually the primary criteria. Special pumps must be used if the dye is to lase in a continuous mode. Certain pumps will not be feasible if the dye laser is to operate at short wavelengths. If very high peak powers are desired, extremely short-pulsed (possibly mode-locked) lasers must be used. In any case, the laser employed must be capable of supplying a useful amount of absorbable power. When a pulsed source is used, it should have a fast risetime and high peak powers. The cw pumps must be very powerful to overcome threshold and triplet state effects. All should be as efficient as possible so that the maximum amount of power is coupled into the dye.

A. DYE LASER PUMPS: A REVIEW

Table I illustrates the various types of dye laser pumps currently being used in the field. It lists the output wavelengths produced by each and a series of references pertaining to the development and application of each. It should be noted that several of the lasers use second harmonic generation (SHG) to achieve wavelengths that can be usefully absorbed by dyes. The flashlamp pump radiates over a wide range of frequencies and hence does not employ

TABLE I

SUMMARY OF DYE LASER PUMPS

LASER	WAVELENGTH (A)	REFERENCES
RUBY	6940	(1) - (3)
SHG[a]	3470	(4), (5)
Nd^{+3} (Glass/YAG)	10600	
SHG	5320	(6) - (9)
THG[b]	3540	
FHG[c]	2660	
FLASHLAMP	Continuous[d]	(5), (10) - (16)
XENON	Numerous[e] 4306 (M) 4954 (M) 5008 (M) 5190 (M) 5260 (S) 5353 (S) 5395 (S) 5956 (S)	(17)
ARGON	5145 (S) 3511 (M) 3635 (M)	(20) - (28)
NITROGEN	3371[f]	(29) - (37)

[a] Second Harmonic Generation

[b] Third Harmonic Generation

[c] Fourth Harmonic Generation

[d] Wide-Band Spectrum

[e] (M) - Medium Strength Line
(S) - Strong Line

[f] Predominant Line

selective absorption. Each of these pumps are briefly described in the sections below. A comparison is provided in the last section.

1. Ruby Laser

The ruby laser was the first pump that was used to observe stimulated emission in a dye. In 1966, Sorokin et al [1]and Schäfer et al [2] used the tremendous output (1000 MW/cm^2) of Q-switched ruby lasers at 694 nm. The resultant lasing action in the dye was observed in the infrared. The above workers employed longitudinal pumping of the dye cell. Concurrently, Spaeth et al [3] used a horizontally spread 694 nm beam to transversely pump a dye laser.

The natural extension of this work was to use a pump with a shorter wavelength in order to observe the dye laser emission in the visible spectrum. Schäfer et al [4] and Sorokin et al [5] reported this in 1967, using a frequency doubler with their ruby lasers. The doubled 10 MW, 347 nm beam was used to pump dyes that lased over the entire visible spectrum.

2. Neodymium Laser

Soon after it was realized that the high power ruby pulses could be used to pump dyes, several workers turned to the powerful Nd^{+3} laser. Its 1.06 micron output lies too far in the infrared to be useful, but McFarland [6] used its 5320 °A second harmonic, in 1967, to pump a

dye. Soon thereafter, Glenn [7] and Soffer [8] were reporting similar results. In 1969, DeMaria et al [9] announced that they had obtained 1 GW peak power (pulse width $\cong 10^{-13}$ sec) pulses from a mode-locked Nd^{+3} laser. Even with a low 0.01% conversion efficiency, the doubled output was immense.

3. Flashlamp

In 1967, while reporting a dye laser using the ruby pump, Sorokin [5] speculated that a fast rising flashlamp could be used to pump a dye laser. In the same issue, in a short communication, he reported that he had pumped four dyes with a coaxial flashlamp [10]. This was the first example of a dye laser that was stimulated with an incoherent source. The flashlamp technology had already existed because of their development for use in flash photolysis. Soon, numerous researchers were reporting flashlamp pumped lasers. They included Schmidt and Schäfer [11], Snavely [12] and Deutsch [13]. The problem of heating in the dye cell had been solved the year before by Schimitschek [14] when he revealed a circulating liquid laser using a flashlamp. In 1968, Sorokin [15] obtained 100 Joule pulses with a risetime of 1 μsec. Drake [16] has improved this to 200 Joule.

In order to maximize the transfer of energy from a flashlamp to a dye cell, several exotic designs have been adopted. Sorokin's device employed a coaxial flashtube-dye cell. Others have used helical lamps or linear lamps that

are elliptically confocal with the dye cell. In all cases, the frequency spectrum of the flashlamp output exceeds the absorption band of the dye. A great deal of radiant energy would be lost unless energy transfer mechanisms are used. This will be discussed in the section on dyes.

4. Xenon Laser

Hänsch et al [17] reported, in 1973, the use of the xenon laser developed by Bridges [18] and extended by Hoffman [19] to pump a dye laser. Hoffman obtained pulses with 390 W of peak power (distributed over four lines) and a pulsewidth of 5 μsec. Numerous lines have been reported, the main ones occuring in the blue and green regions (e.g. 430.6, 495.4, 500.8, 519.0, 526.0, 535.3, 539.5 and 595.6 nm). Hänsch claimed a dye output of 10-20 W peak power with pulse widths of 0.3 μsec. Krypton has also been used in the same manner as xenon. The notable characteristic of these pulsed ion lasers is the large number of discrete lines spanning the visible spectrum. Only limited use of these lasers as pumps has been reported, however.

5. Argon Ion Laser

Peterson et al [20] reported in 1970 the first example of a cw dye laser. They used the 5145 Å output from a 1 W argon ion laser to pump the dye and employed a triplet quencher to maintain lasing. Since that time, the argon ion laser has been used extensively by a large number of researchers. Many of the articles report unique methods

of coupling the pump beam into the dye with as little loss and as much beam focusing as is possible [21]-[28]. The average powers being used today is 3-4 W.

6. Nitrogen Laser

In 1969, Lankard and von Gutfeld [29] revealed that they had used a 100 kW commercial molecular nitrogen laser, radiating at 3371 Å, to obtain laser action in two dyes. Almost immediately, many articles appeared reporting a variety of experiments using the nitrogen laser as the optical pumping source [30-35]. Nearly all of these arrangements used transverse pumping of the dye cell. The reason for this rush to use the nitrogen laser is obvious: The output pulses are very narrow and have high peak powers and the laser radiates in the ultra-violet, thereby extending the range of dyes that can be pumped. Its cost is also minimal compared to the other pump lasers available at these wavelengths. Since this introduction, a great deal of effort has been expended in attempting to improve the pulse shapes and peak powers. Recently, Goddard [36] announced that he had constructed a nitrogen laser with a 9 MW output. This figure is open to debate and will be discussed in a later section. To date, an efficiency of less than one percent is considered normal. Most of the current commercial nitrogen lasers have powers ranging from 50 to 500 kW. Recently, Willett [37] reported that he had doubled the output of nitrogen lasers by the addition of small amounts of SF_6.

It was later learned that this additional gas causes a residue of sulfur to accumulate in the laser. It may be possible, however, to find another gas which will improve the output without fouling the laser.

7. Comparisons

The ruby and neodymium lasers in themselves are quite limited for dye laser pumping purposes because of their long wavelengths. Dyes pumped by these sources lase only in the infrared. By frequency doubling or tripling the outputs, very powerful beams at useful frequencies can be obtained. Harmonic generation, however, requires large amounts of power to obtain the SHG beams. The overall effect of this is to make the apparatus large and expensive to purchase and operate.

The flashlamp has many attractive features. It is compact, provides multi-Joule outputs and can be constructed for almost any application. For these reasons, it is widely used by teams with available finances. The flashlamp has two main drawbacks. Since it radiates over a wide frequency range, much of the lamp energy is not usefully absorbed and this fact reduces the efficiency of the device. Efforts are being made to incorporate energy transfer mechanisms in the dye to use all of the pump radiation. In addition, the flashlamps possess a limited number of available shots before they break down. The apparatus that is associated with flashlamp pumped dye lasers — precise reflectors, heat dissipators, etc. — require exacting tolerances.

As was stated earlier, the xenon laser is used only sparingly as a dye laser pump. Its low divergence beam is ideal for use in end-pumped dye lasers, but the low output peak power and middle frequency range limits the versatility.

The argon ion laser is used exclusively to pump the cw dye laser. The purchase cost is high and the device requires a large power input. For dye laser frequencies less than 5000 Å, the moderate-to-weak 3511 and 3635 Å lines must be used. These "deficits" are usually overlooked as this laser is, with minor exceptions, the only practical cw pump available.

The molecular nitrogen laser is attractive for several reasons. It can be purchased for moderate prices or constructed in the laboratory. It possesses high peak powers and short pulsewidths. The nitrogen laser does present a few problems, though. The efficiency of the laser is quite low, usually less than 0.1 percent. The ability of power supplies to furnish current can restrict the repetition rates. These rates decrease further when larger amounts of energy are called for in the laser. The narrow pulsewidths also present oscillation problems which must be resolved by minimizing inductances and unnecessary capacitances in the charging circuits.

In the studies pursued in this paper, the firing rates are not critical and ringing could be reduced to an

acceptable level. The nitrogen laser's pulse characteristics are very desirable for spectroscopic work and the laser parts could be constructed locally. It was therefore decided to analyze the various nitrogen laser designs reported previously and attempt to build a laser incorporating the best features of each. It was hoped that acceptable powers at a reasonable cost could be obtained.

B. THE NITROGEN LASER: THEORY

In 1963, Heard [38,39] reported a strong laser line at 3371 Å emanating from a pulsed nitrogen-gas laser he had constructed. This laser had such a large gain that only one mirror was used (so as to avoid losing half the available power). The nitrogen laser demonstrated a fast risetime, narrow pulsewidth and high peak power. Given this, though, it wasn't until six years later that it was used to successfully pump a dye laser.

In his original articles, Heard correctly identified the transition responsible for lasing as $C^3\Pi_u \rightarrow B^3\Pi_g$ (see Figure 1), but he did not speculate on the origin of the inversion in these triplet states. Leonard [40] and Gerry [41] performed the first experimental studies of the processes involved. Leonard determined that an E/p of about 200 V/cm-torr provided an optimum output over a wide range of pressures. He also investigated how the length of the active gain region affected output. Leonard found that for discharge lengths up to 80 cm, the gain was

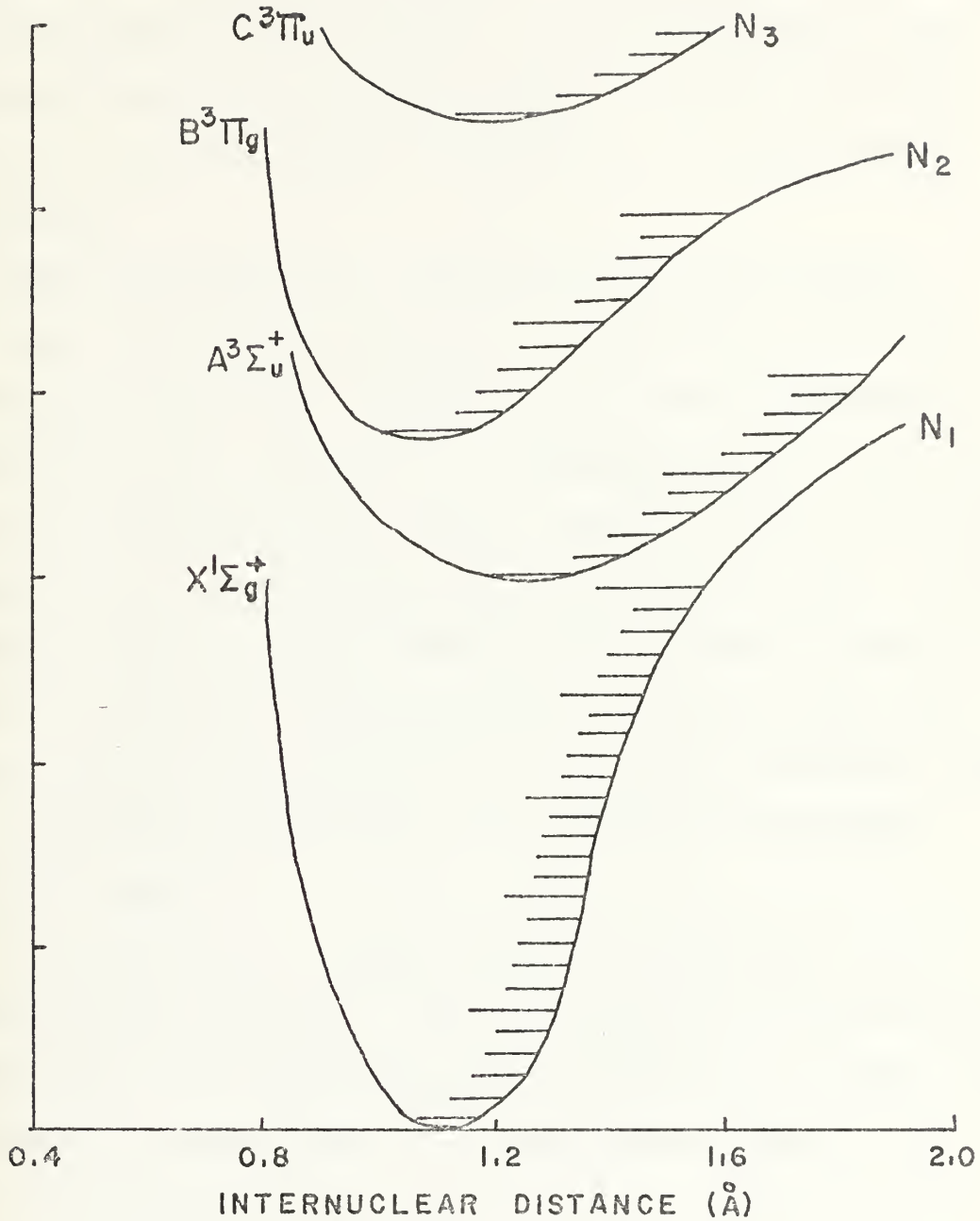

POTENTIAL ENERGY DIAGRAM FOR MOLECULAR NITROGEN (GODARD)

FIGURE 1

75 dB/m (3×10^7/m) and that for greater lengths, the output saturates and the gain becomes linear with length. Gerry concluded that the excitation mechanism resulting in the inversion was the product of the direct electron impact excitation.

Since the radiative lifetime of C is approximately 40 nsec., this direct excitation overpopulates the upper lasing level for this lifetime before lasing destroys the inversion with B. State B is a metastable state (and hence does not depopulate very rapidly) since a triplet to singlet transition is involved in decay to the ground state. Gerry used the ratio of Franck-Condon probabilities to determine that the excitation cross section of C was at least ten times that of B and stated that this direct excitation was the predominant mechanism in the pumping of the second positive band (C).

Ali et al [42] extended Gerry's calculations to cover nonsaturation conditions. The rate equations and derivation which follow are essentially those used by Ali. Since the molecular nitrogen laser is a three level system:

$$\frac{dN_3}{dt} = X_{13}N_1 + X_{23}N_2 - (Y_{31} + Y_{32} + \tau_{31}^{-1} + \tau_{32}^{-1})N_3$$
$$-R_{32}^{i}(N_3 - (g_3/g_2)N_2) \qquad (1)$$

$$\frac{dN_2}{dt} = X_{12}N_1 + (\tau_{32}^{-1} + Y_{32})N_3 - (\tau_{21}^{-1} + Y_{21} + X_{23})N_2$$

$$+ R_{32}^{i}(N_3 - (g_3/g_2)N_2) \qquad (2)$$

$$\frac{dN_3}{dt} = -(X_{12} + X_{13})N_1 + (\tau_{21}^{-1} + Y_{21})N_2$$

$$+ (\tau_{31}^{-1} + Y_{31})N_3 \qquad (3)$$

where:

N_1, N_2, N_3	=	Population densities of ground, lower and upper levels, respectively
X_{ij}	=	Rate of collisional excitation by electron impact from level i to level j
Y_{ji}	=	Rate of collisional de-excitation from j to i
$(\tau_{ji})^{-1}$	=	Rate of radiative decay from j to i
R_{ji}^{i}	=	Rate of induced emission
g_3, g_2	=	Statistical weights of upper and lower lasing levels.

In his calculations, Ali made the following assumptions: N_1 is constant (large number in ground state compared to other states), $\tau_{31} >> \tau_{32}$ (since C is metastable with respect to ground), $X_{13} >> X_{12}$ (as postulated by Gerry), $\tau_{21} >> \tau_{32}$ (B is metastable with respect to ground -- τ_{32} = 40 ns and τ_{21} = .1 μsec.), and $Y_{31} = R_{32}^{i} = 0$. Ali

concluded the following:

$$2/(Y_{32} + \tau_{32}^{-1}) > t \quad \text{for } N_3 > N_2 \tag{4}$$

which states that the inversion must be established in a period of time that is shorter than the upper state lifetime (even when $Y_{32} = 0$). This is of critical importance in the design of the nitrogen laser.

Ali also determined that the fields present in the discharge were as important as the pulse risetimes. He analyzed the effect of Y_{32}, the collisional deactivation term, and found that if the fields were not large enough to impart at least 6 eV to the electrons, a great deal of the available energy is lost to vibrational absorptions and de-excitations by collisional mixing. In this way, he supported Leonard's 200 V/cm-torr figure. For these reasons, the nitrogen laser design should aim at attaining large fields in a very short period of time.

The long lifetimes of B also presents problems. The gas must flow through the laser rapidly enough to replace the "hot" gas between pulses. These gases also contain a great number of molecules which have been promoted to a higher vibrational state and tend to decrease the amount of radiation at 3371 Å.

C. THE NITROGEN LASER: EXPERIMENTAL

The requirements for high discharge fields and fast risetimes impose severe limitations on the design of nitrogen lasers. The 40 ns pulsewidth corresponds to a frequency of 4 MHz. This frequency range is not uncommon in the capacitive-inductive circuits employed in the laser construction. Almost all of the present laser designs go to great lengths, primarily by using low inductance transmission line (Blumlein) configurations, to minimize ringing and oscillation. Most of the devices also use capacitors to store large amounts of charge which is then rapidly transfered to the laser electrodes by some triggering mechanism. Numerous articles on the construction and improvement of the nitrogen laser exist [45-50].

During the course of this study, two nitrogen lasers were built and a previously constructed model was modified and its performance was optimized. These will be called the Nagata, Schenck and Godard designs and will be discussed in the order that they were constructed or utilized.

1. The Nagata Design

In 1973, Nagata and Kimura [51] reported a "compact high-power nitrogen laser" using a cross field, low impedance laser configuration in a transmission line format. Its small size, relatively high power and ease of construction was immediately appealing and it was therefore chosen for the initial attempt in constructing a laser that would efficiently pump a dye laser.

The Nagata laser is represented in Figure 2 and the circuit schematic is shown in Figure 3(A). The transmission line was constructed of 1/8 inch copper plates spaced 1-1/2 inches apart. Ten 500 pF doorknob capacitors were mounted on each side of the laser cavity and helped to maintain the plate parallelism. The upper plates formed the cavity electrodes. Stainless steel strips were soldered onto the discharge edges of the plates to avoid sputtering and prolong plate life. These electrodes were 38 cm long. The edges of the electrodes were placed exactly 20 mm apart and held in that position by the screws into the capacitors. The laser cavity was then formed by mounting Plexiglas strips above and below the electrodes. 1/16 inch quartz windows sealed the ends and Plexiglas strips sealed the sides not in contact with the electrodes. Holes in the top of each end provided for nitrogen entrance and exit ports. The charging inductor was constructed from 20 turns of #12 gauge wire coiled into a helix with an inner diameter of 1/2 inch.

The spark gap was mounted directly to the upper and lower plates. The spark gap geometry was as shown in Figure 4(A). The entire assembly was mounted in a Plexiglas box and nitrogen was flowed slowly through the spark gap cell.

The circuit operation was as follows: A positive voltage was applied to the plate opposite that of the spark

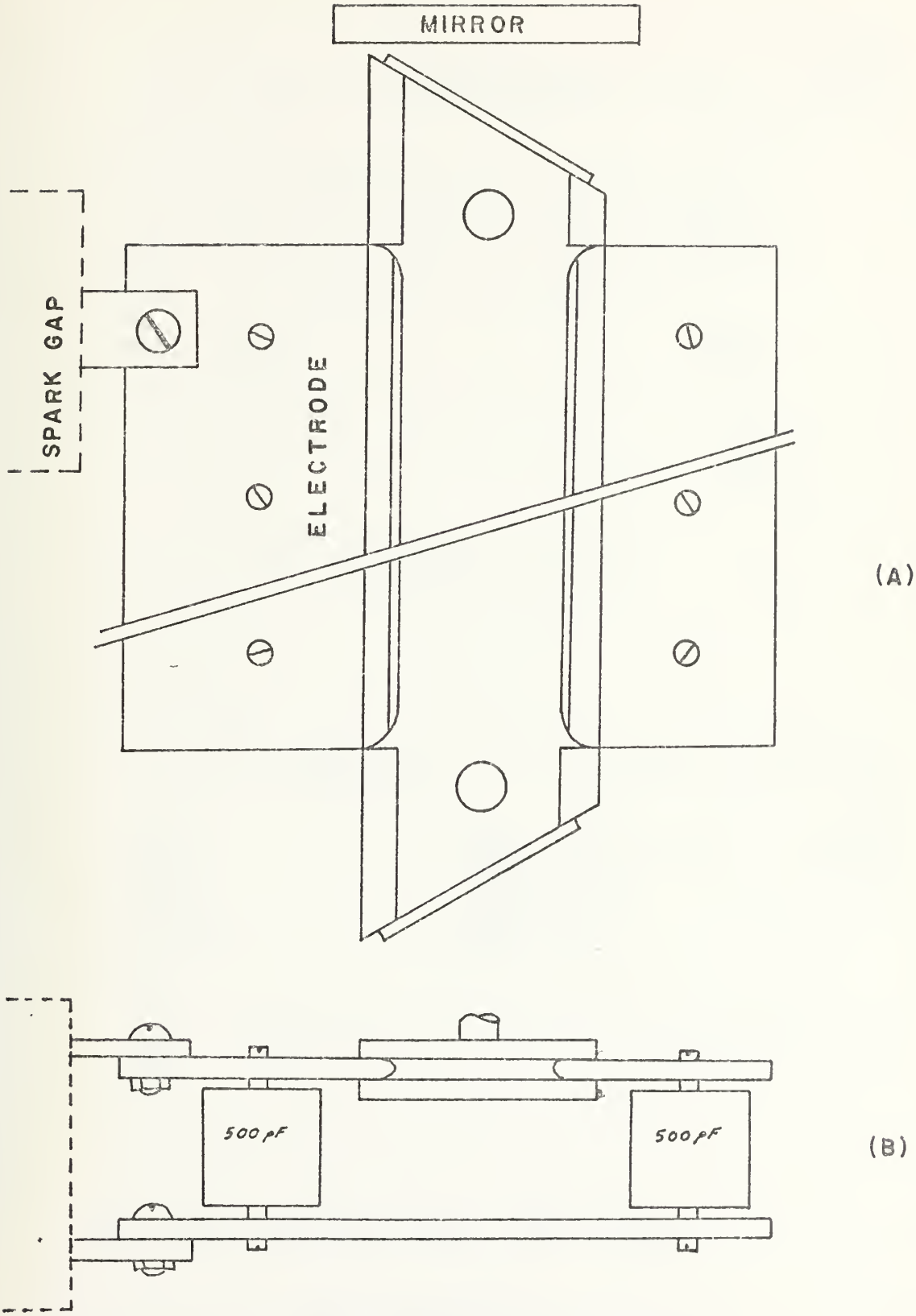

NAGATA LASER

FIGURE 2

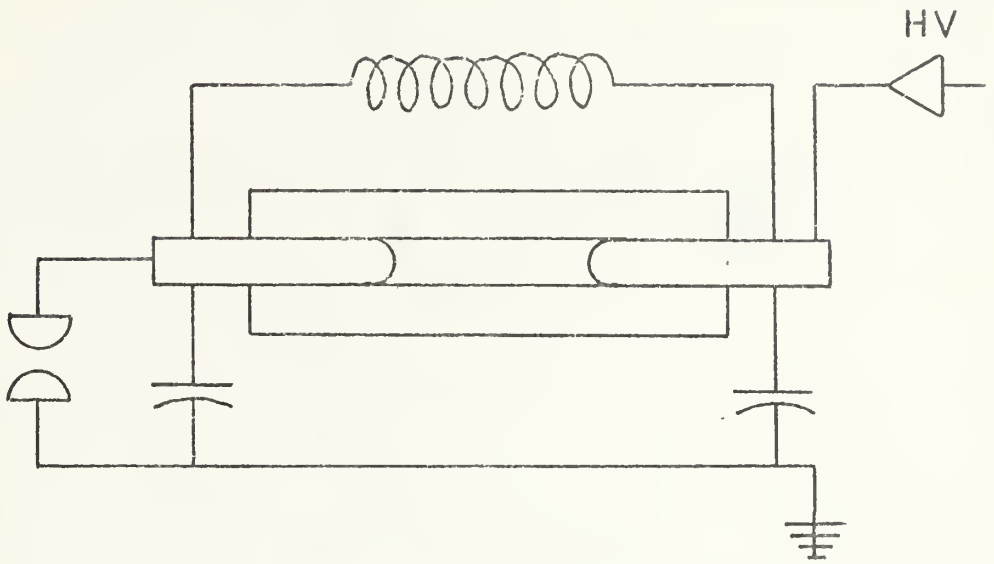

(A) NAGATA LASER

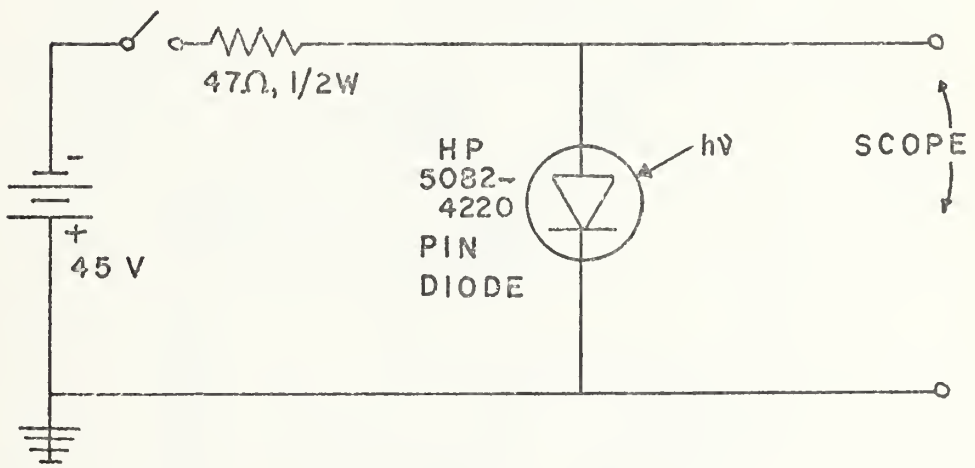

(B) PHOTODETECTOR NETWORK

SCHEMATICS

FIGURE 3

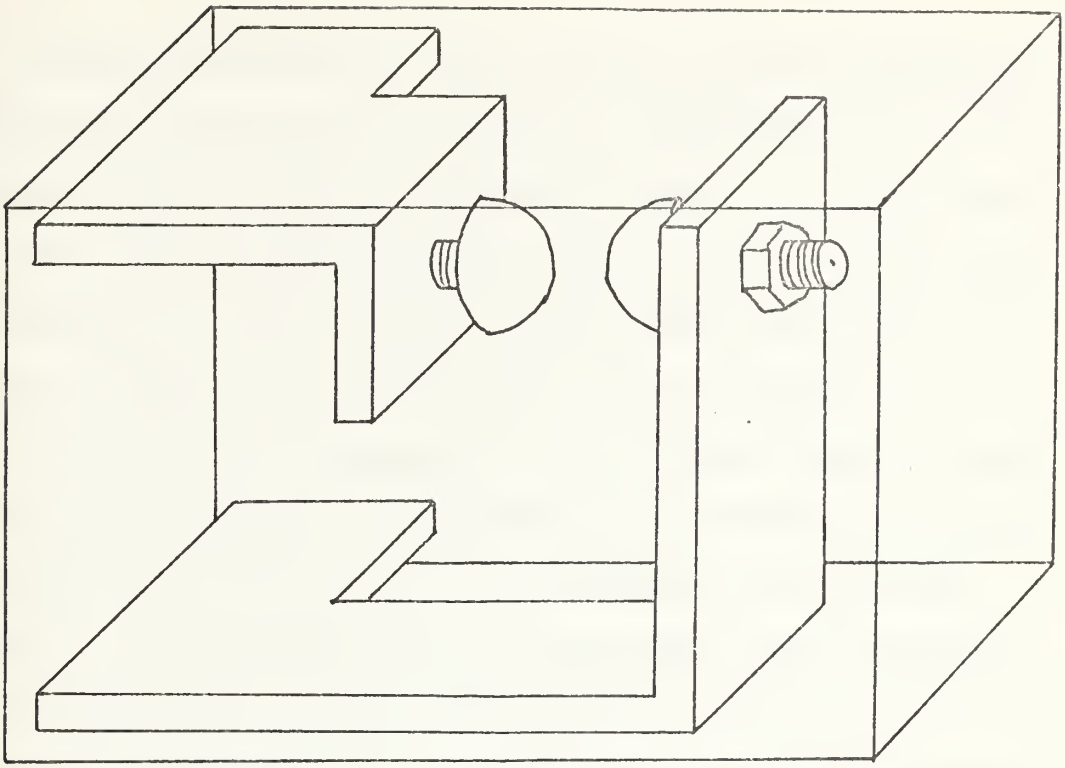

(A)

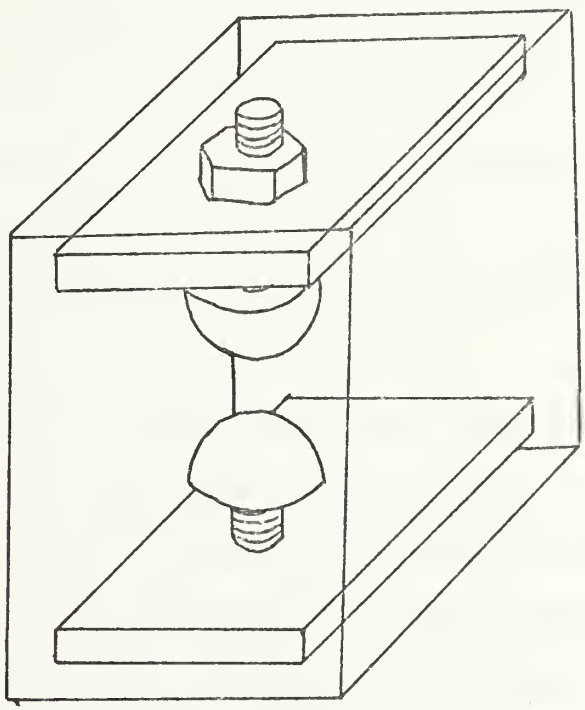

(B)

NAGATA LASER SPARK GAPS

FIGURE 4

gap. Since the charging cycle occured at low frequencies (1-100 Hz), the inductor across the electrodes had a low impedance and allowed both plates to charge. Both sides of the laser cavity were then charged to the spark gap breakdown potential. As soon as the spark gap arced over to ground, a wave at the ground potential proceeded from the point of arcing. If the spark gap is placed near the rear edge of the electrode, the discharge gap nearest the spark gap first will see a large, rapid potential difference across it. This difference initiated the field generated electron discharge across the nitrogen medium. As the drop to ground proceeded away from the spark gap, the discharge proceeded down the laser tube. Since the drop to ground potential was very rapid (~ 10 ns), the inductor had a very large impedance and was, effectively, an open circuit, allowing the potential difference to be achieved equally along the entire length of the laser tube. The power supply was constantly providing energy and the circuit began to recharge immediately.

An unregulated power supply provided up to 15 kV to the plates. Its limited ability to supply large amounts of current allowed only a moderate repetition rate. The high voltages (14.5 kV) provided, however, enabled the laser to impart .525 J of energy across the electrode gap.

A low divergence, ultraviolet beam was detected coming from the laser the first time it was fired. When

the beam was focused into a dye cell, the dye fluoresced brightly, but it did not appear intense enough to enable the dye to commence lasing action. This conclusion was based on previous observations of dye lasers in operation. When a power meter or oscilloscope was brought into the room in order to measure pulse characteristics, the RF radiation being emitted from the spark gap and its associated circuits foul their triggering sections. The beam had to be focused into an adjacent room in order to avoid this problem. A biased HP 5082-4220 PIN Photo-diode was used to measure the pulse shape. Its circuit schematic is shown in Figure 3(B). The FWHM pulsewidth was ~ 10 ns. A JODON PM-550 power meter provided a measure of the integrated power output. Initially, it read 0.02 mW. We estimated a repetition rate of 3 Hz. This initial attempt showed that the approximate peak power was only about 667 watt. This was much too small to pump a dye laser.

One of the features noted in the laser discharge was the bright arcing at both ends of the electrodes. Several attempts were made to suppress this arcing. The corners were rounded as much as possible and all edges were made spherical. Even though power increased to 3.3 kW, the arcing persisted even when Teflon and plastic tape were placed over the ends. It was also noted that the Plexiglas plates were becoming deeply etched and carbonized, thereby providing a low impedance path for the arcing. These "tunnels"

were filled with RTV cement filler and one of the electrodes was replaced with a band saw blade embedded in a copper plate. Although the arcing continued to a lesser extent, the power was raised to 9 kW.

During the measurements of pulse widths, considerable ringing of the RF radiation had been noted. It was believed that the severe angles and partial loops in the existing spark gap may have been responsible for this. A new spark gap was constructed which had a minimum number of corners and leads. This new design is shown in Figure 4(B). It was mounted as close to the plates as possible and again flooded with nitrogen. Concurrently, the Plexiglas cavity plates were replaced with glass in order to alleviate the carbonizing and bridging by the arc. This required a shift of the inlet and outlet plugs to the side of the tube, adjacent to the electrodes. All leads were minimized and straightened. The original electrode replaced the band saw blade. These combined alterations reduced the pulsewidth to 6-7 ns. The laser, at this point, emitted a pulse with a peak power of 24.3 kW. In all cases, it was found that the optimum output occured for an E/p of about 180 v/cm-torr which is very close to Leonard's value. Under optimum conditions, and using a limited number of dyes, lasing was then theoretically possible. Since CARS studies require the use of two dye lasers and further large increases in output power was considered unlikely, other nitrogen laser options were investigated.

2. The Schenck Design

Schenck and Metcalf [52], in 1973, unveiled a large powerful nitrogen laser that could also be constructed by laboratory personnel. It was known that the Electrical Engineering Department had such a laser. It was understood, however, that this device was inoperative. An investigation showed that the pulse generating circuit had been wired wrong and this was repaired.*

The Schenck laser is shown in Figure 5. There were several basic differences between this and the Nagata design. A thyratron was used instead of a spark gap and the capacitor arrangement was different. The use of a thyratron enabled the laser to be triggered by an external source which could be accurately varied to any specific repetition rate. This was important if very accurate measurements of peak power were to be made.

The sequence of events resulting in the discharge was as follows: A power supply placed up to 20 kV on the floating storage capacitor. When the thyratron was fired, the side of the capacitor nearest it went to ground potential and much of the charge on the storage capacitor was transfered to the dumping capacitors. These established a

---

*A special thanks to Lt. J. Jaques for his help in restoring this system and to Professor J. P. Powers for allowing us to use this system.

(A)

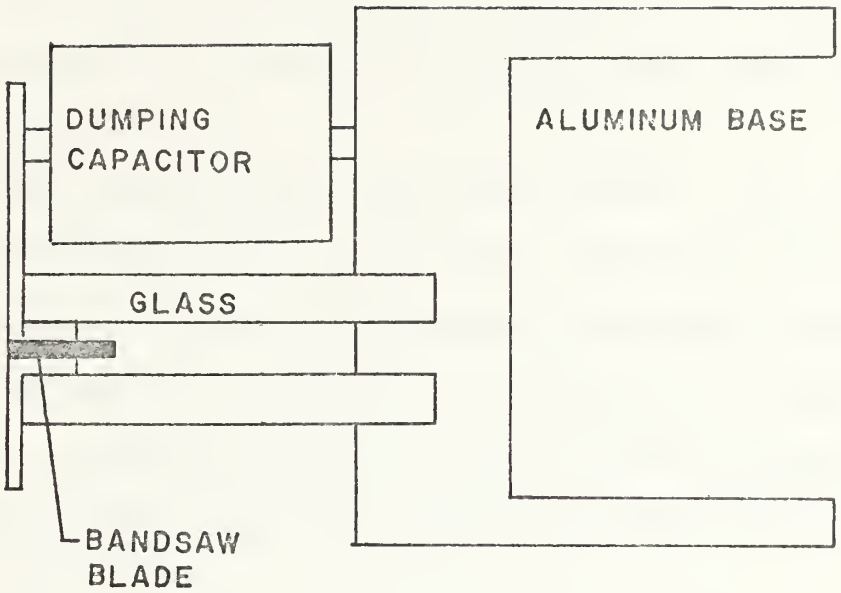

(B)

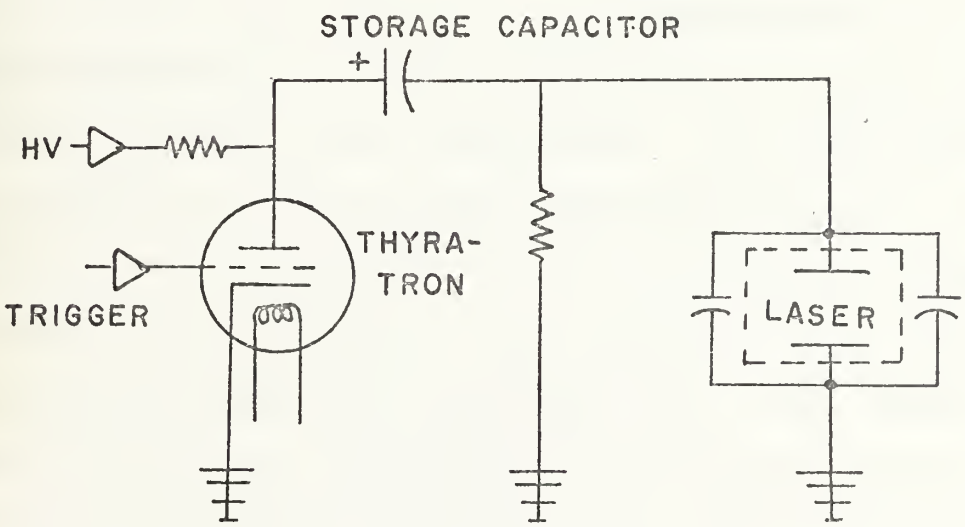

SCHENCK LASER

FIGURE 5

field across the laser channel and a discharge resulted. Although the actual firing sequence was different from the Nagata laser, both designs were basically the flat-plate transmission line, Blumlein pulse generated laser proposed by Shipman [43].

The Schenck laser that was used was 1.25 m long and the laser channel was 3.81 cm wide. The laser also used a sawblade to create a more uniform discharge. A maximum peak power output of 65 kW was obtained over a range of 1-60 Hz. Although this laser was 3.26 times longer than the Nagata laser, the output power was only 2.67 times as great.

It was observed that the pulse widths from the Schenck laser were ~ 10 ns long or longer, thereby reducing the peak power. Some time later, a solid copper bar was used to replace the wire leads from the storage capcitor to dumping capacitors and the entire electrical network was condensed to reduce stray inductances. The pulse widths were reduced to 8-9 ns giving a peak power of 81 kW. The laser was operated at 20 Hz, 15 kV and 48 torr. It should be noted that the first dye laser action here was obtained using this nitrogen laser pump and a very crude optical cavity. With care, superradiant lasing action could be achieved using the more powerful dyes. Although the output powers from this laser were very respectable, it was still inadequate for simultaneously pumping two dye lasers to powers high enough to be useful in CARS.

3. The Godard Design

In 1974, Godard [36] published an article stating he had constructed a traveling wave nitrogen laser which had an output of 9 MW and an efficiency of 1%. These large figures were startling and many people attempted to duplicate them. The basic design is shown in Figure 6(A). Godard's laser also employed a flat plate transmission line in Blumlein configuration. It used a dual sided sheet of printed circuit board, 24 inches wide by 48 inches long. The material between the sheets of copper acted as the dielectric and both sides of the discharge channel were essentially continuous capacitors. The bottom was a solid sheet of copper while the top had a channel 2 inches wide etched across it. A 2 inch strip on top and bottom had been etched around the entire circumference to preclude edge-over arcing. A sample piece of this material with a 2 inch etched border withstood 40 kV before it arced over. Figures 6(A) and 7 show the construction of the laser cavity. A glass plate was placed over the etched channel on the board. This was done to protect the dielectric from being damaged by fragments of hot metal. It also tended to raise the level of the discharge. This was necessary to clear the bottom of the end windows.

Two heavy brass electrodes were placed on top of the copper cladding on each side of the channel. These were milled so as to fit the glass plate. Their weight

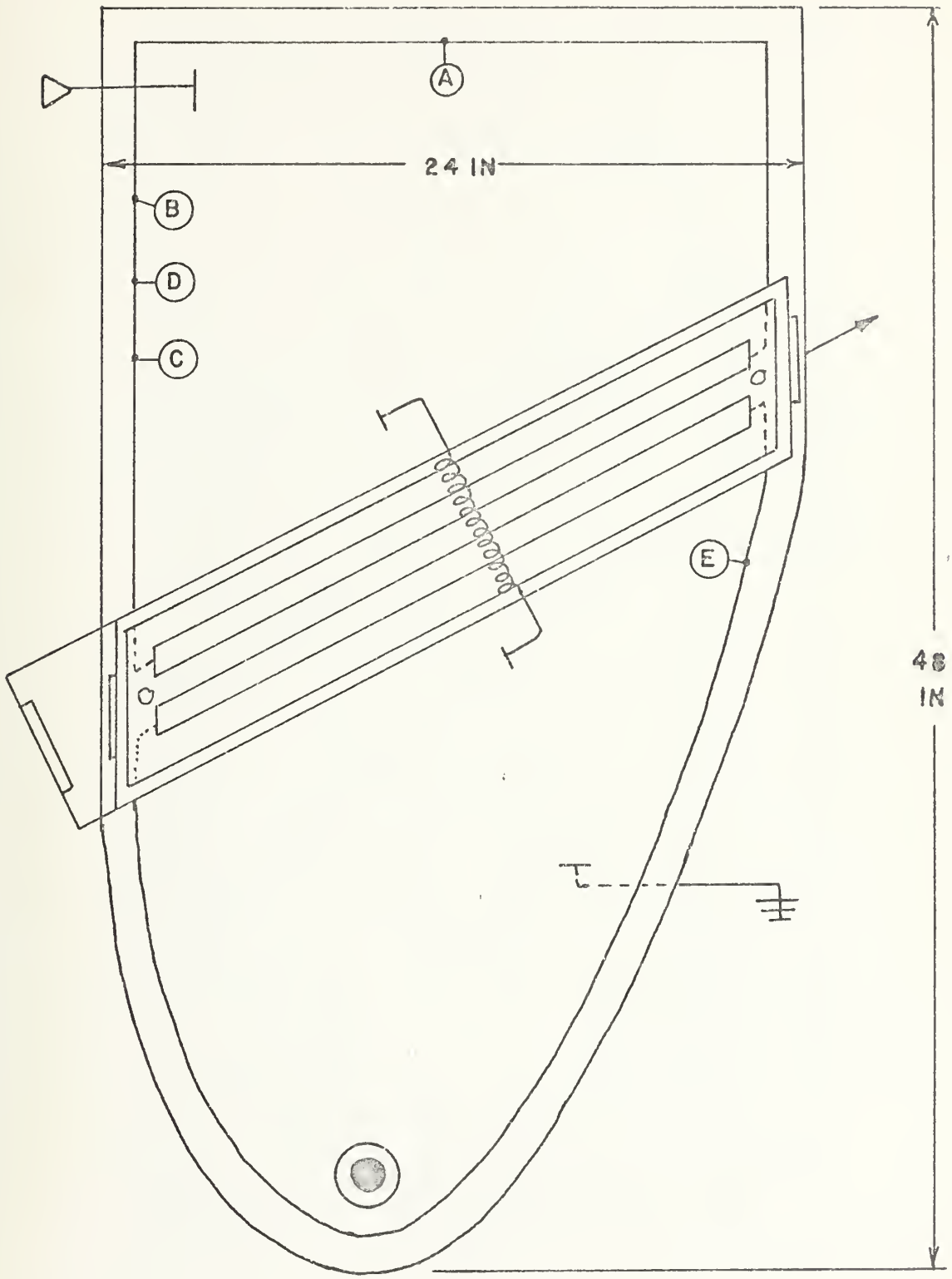

GODARD LASER

FIGURE 6(A)

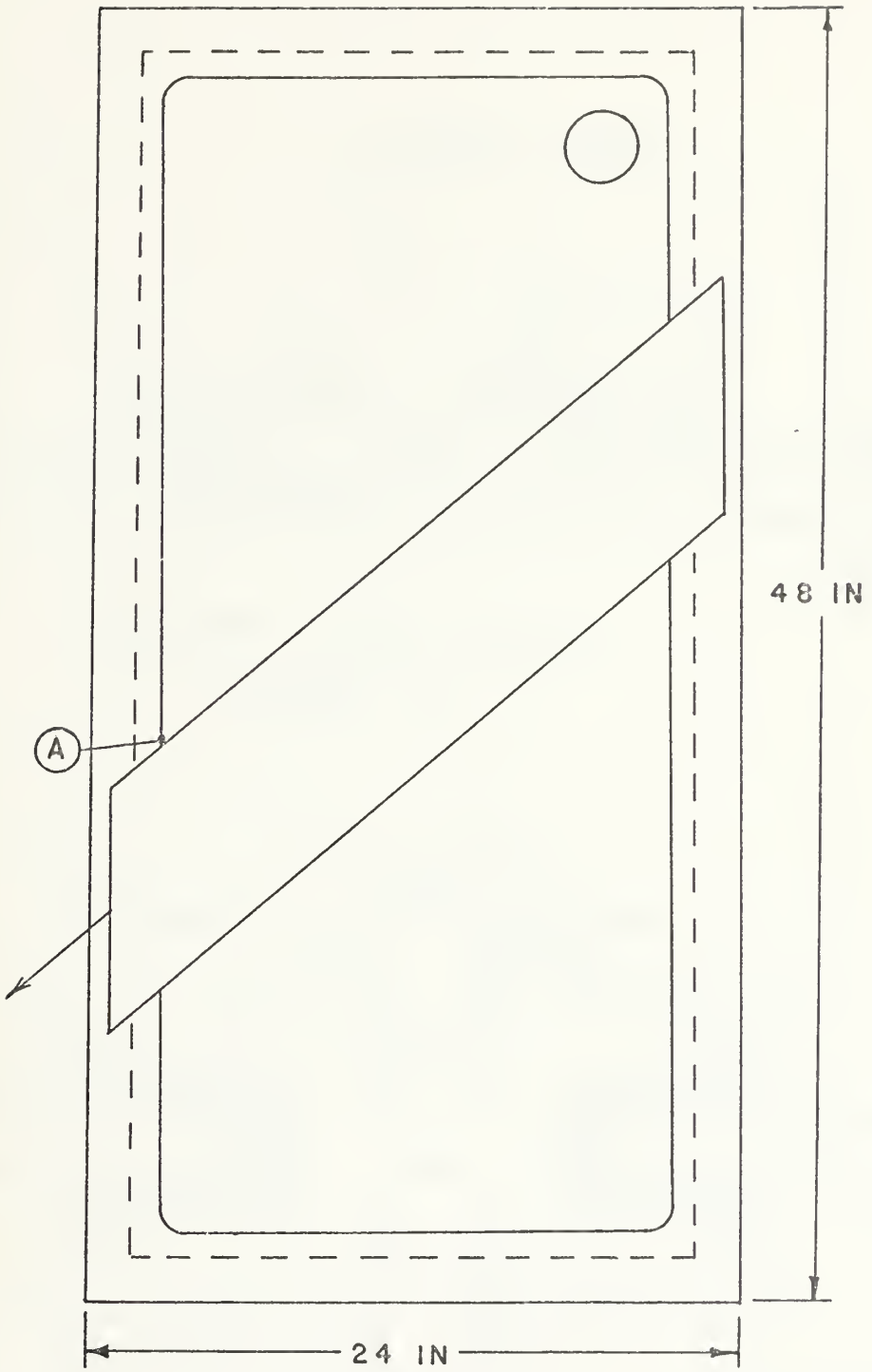

MODIFIED GODARD LASER

FIGURE 6(B)

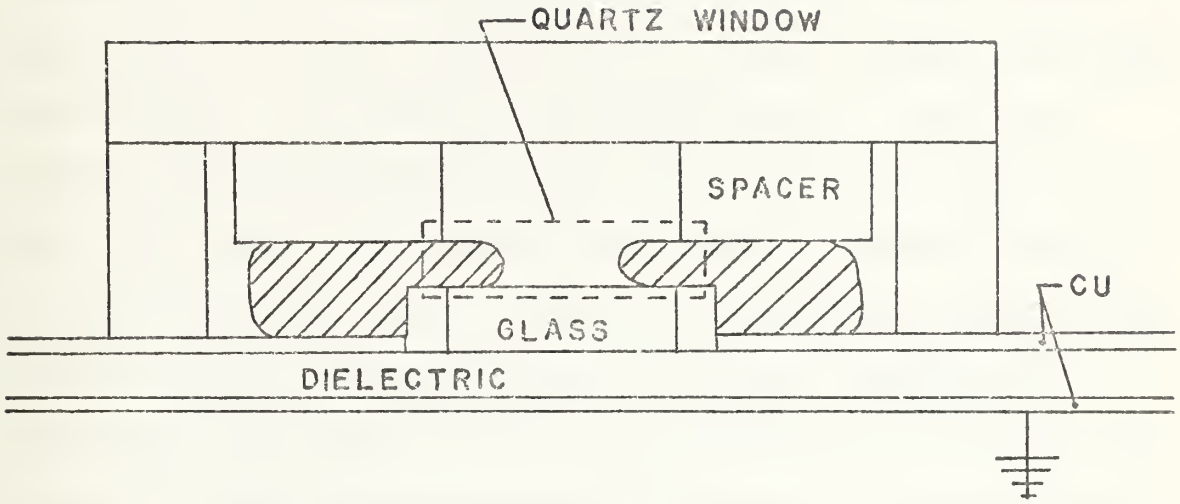

GODARD LASER CAVITY

FIGURE 7

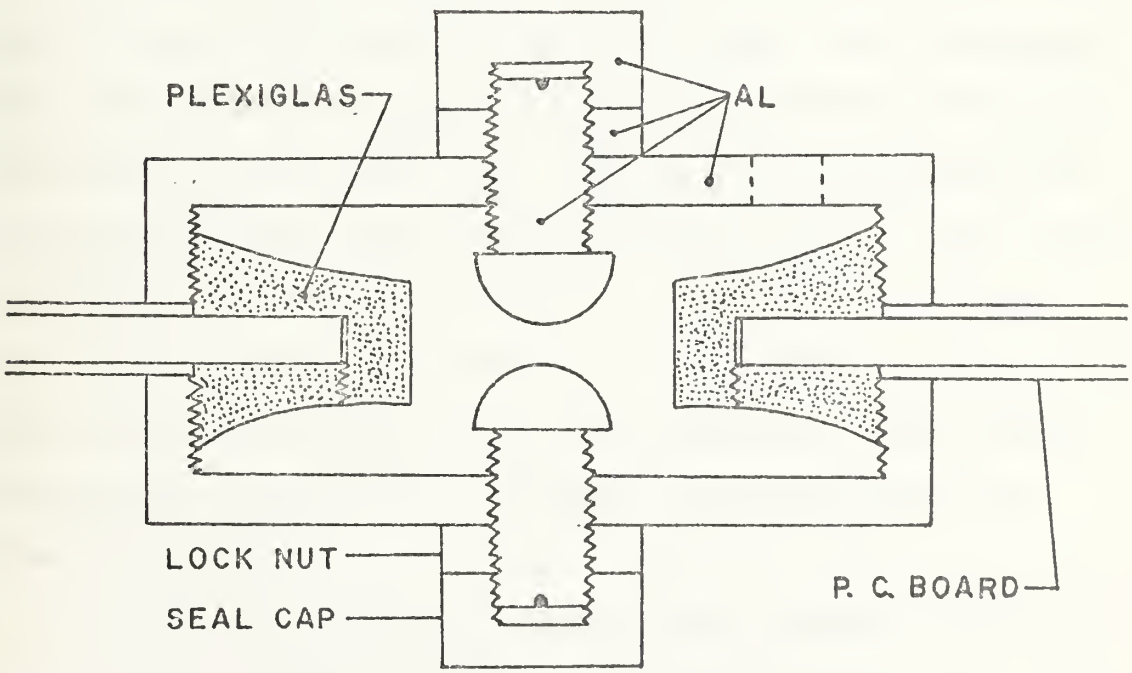

GODARD SPARK GAP

FIGURE 8

provided for the contact between the electrodes and the copper. A Plexiglas box was then fitted over the entire assembly. The bottom edge of the box had a thin, smooth, dry coat of silicon cement which had been covered with stopcock grease. This made a good vacuum seal. 1/16 inch quartz plates were fitted over holes drilled in the end of the box. They were attached with paraffin which also provided an airtight seal. Two lead bricks were placed on top of the box to facilitate proper sealing. Nitrogen was admitted at the top of one end of the box and drawn out by a vacuum pump at the top of the other end. When the pressure in the box was reduced, the seals all tightened up and the box could be evacuated to fairly low pressures.

Since the substrate material was quite thin, the high vacuum would easily implode the area under the glass. For this reason, Plexiglas spacers were inserted between the electrodes and the box. In this way, the electrodes were forced down (making more positive contact) and thereby reinforced the bottom structure. The open area between the spacers above the electrodes also tended to channel the nitrogen gas along the top of the electrodes and reduced considerably the area that needed to be supplied with fresh gas.

An inductor coil, with an inner diameter of 1/2 inch, was constructed of 20 turns of #12 gauge wire. It was mounted from one side of the copper cladding to the

other, over the cavity box. In order to avoid possible weakening of the dielectric by heating effects, the ends of the inductor were soldered to small copper sheets which were tightly taped to the copper cladding. The power supply line was similarly attached to the end opposite the spark gap and the ground lead was attached to the copper cladding on the bottom.

The spark gap was designed and machined to be small and efficient and to have the minimum possible inductance. It is shown in Figure 8. A 1 inch hold had been drilled through the board at the apex of the parabola. The copper on both sides was then etched back 3/4 inch. The two threaded plastic sides served both as anchors to the board and as a dielectric to prevent premature arcing from one side of the board to the other. Metal caps with electrodes were then screwed down onto the copper, making solid contact with the cladding on both sides. The electrode spacing could be adjusted by turning the threaded electrodes. Nitrogen was admitted through a brass fitting and leaked out through the threads.

The operation of the Godard laser was nearly identical to the Nagata laser. The two sides of the laser cavity were charged to the same voltage via the coil. When the spark gap reached its predetermined voltage, it arced over and the top part of the spark gap went to the ground potential. Because of the parabolic shape of the transmission

line/capacitor, a plane wave at the ground voltage proceeded towards the electrodes. The end of the electrode nearest the spark gap first saw the drop and it was here that the field across the cavity first appeared and emission commenced. As the wave continued, the discharge proceeded down the cavity and emission along the laser tube was preferentially spontaneously induced, with only minor emission in other directions. The mirror served only to salvage radiation traveling in the back direction.

The sequence described above is the theoretical reason for the shape of the circuit board, as explained by Godard. Several measurements were made of the laser output in both directions out of the cavity. For example, in one case, it was found that .62 mW integrated power was emitted in the forward direction and .61 mW in the reverse direction. Addition of the mirror increased the power to 1.7 mW in the forward direction. Hence, no evidence of the traveling wave effect that was claimed by Godard could be seen. Powers up to 160 kW have been obtained from this laser. The capcitance of the board can be found:

$$C = \frac{\kappa \varepsilon_o A}{d}$$

where:

$$\kappa = 4.8$$

$$A = .37 \text{ m}^2$$

and is found to be .021 μF. Since

$$E = \frac{1}{2} CV^2,$$

with V = 12.5 kV, the input energy per pulse is 1.64 J. A peak power of 160 kW in a pulse 8×10^{-9} sec long gives 1.28×10^{-3} J per pulse output. Therefore, the overall efficiency is .08%. This is well below the 9 MW, 1% laser claimed by Godard. Recent discussions with several leading researchers and the literature verify these lower efficiencies [50,53].

One tremendous advantage that the Godard laser had over other designs was the ease with which the entire apparatus — spark gap, cavity cover, electrodes — could be disassembled, cleaned, altered and reassembled. With some practice, it could generally be done in less than an hour. Electrode spacings of 12.5, 15 and 19 mm have been tried with corresponding pressure changes and have verified the optimization condition. Peak powers were obtained for E/p of 200 V/cm-torr ± 10%. This ease of assembly and disassembly allowed various aspects of the laser design to be changed and the resulting effects investigated.

The power supply used with the Godard laser was a full wave rectifier built in the laboratory. It used a neon sign transformer as the voltage producing element and a diode bridge to rectify the output. A large capacitor

was used to smooth ripple. Because of the limitations of the transformer, only 10 kV could be obtained from this unit.

Since the laser output power is proportional to the square of the applied voltage, it is obvious that an increase in the size of the power supply would be an immediate way to increase the laser power. To this end, the unregulated high-voltage supply, used with the Nagata laser, was attached to the Godard laser. The spark gap and nitrogen pressure was adjusted and the laser was fired at 19 kV. The repetition rate was 2-3 Hz. This high voltage caused a number of bright arcs to occur in the discharge cavity, but they moved up and down the length of the cavity, rather than becoming isolated in one or two specific locations, as in the Nagata laser. The laser was also much noisier than it was at 10 kV. The intensity of the output appeared to be considerably higher (as demonstrated by an increase in the output of the two dye lasers) but before the 3371 Å output could be measured, the laser broke down with a sharp, loud snap. It was determined that the voltage had arced over from one of the electrodes of the spark gap, through the larger Plexiglas spark gap retainer (thereby destroying it), to the opposite polarity copper cladding. It was believed that the stress, caused by the tightening of the anchors together, along with the high voltage, was responsible for this breakdown.

A new anchor part was machined from nylon stock and the spark gap was reinstalled on the board. The operating voltage was reduced to 16 kV and the laser was again fired. The electrode spacing was increased to 19 mm in order to reduce the arcing in the laser cavity. As before, a small number of constantly shifting arcs were observed. Also, the noise that accompanied the discharge was considerably louder than in the case with the lower voltages. The laser had been running at 2-3 Hz, 16 kV for about half an hour when a loud noise was heard and the laser ceased operation. It was immediately apparent that a short had occured in the dielectric board on the edge of the cladding, as shown by Point A on Figure 6(A). In an attempt to salvage the remainder of the board, the end of the PCB was cut off along the cladding edge and that end was re-etched back 1 $\frac{1}{2}$ inches. Concurrently, the sparking voltage was reduced to 14 kV and the laser was turned back on.

After 15 minutes of operation, another hole occurred on the board at Point B. The side could not be cut off as before, so another method was attempted. A two inch semi-circle of copper around the hole was etched, with nitric acid, from the top of the board. Q-Putty was used to dam off the etching area. The rough hole was drilled out to 3/32 inch and the whole region was covered with silicon cement. The spark gap was adjusted to spark at 12.5 kV and the laser was again turned on. A short time later,

another hole appeared at Point C and the laser stopped. Since all three breakdowns had occured near the high voltage input, it was felt that its corner location may have induced some form of constructive interference. The high voltage input was moved to the center of that side of the sheet and the hole was repaired as described above. After operating at 12 kV for 15 minutes, another hole appeared at Point D. It should be pointed out that none of the new breakdowns occured at places that were involved in the repair of previous breakdowns.

All of the holes had appeared along the edge on one end of the laser board and this discontinuity at the edge may also have contributed to the difficulties. To alleviate this, the top of the square end of the board was etched back 1 inch all around the periphery so that the top and bottom edges didn't coincide. The parabolic end was left as it was. The hole was repaired and the laser was again turned on. The voltage was set at 10 kV and it was increased by 1 kV increments until it was operating at 16 kV, where it was kept for 2 hours with no further destruction. It might be noted that the spark gap cover became quite warm during this operating time.

A second board had, by then, been completed so, the next day, it was decided to continue elevating the voltage to see how the board responded to the recent modifications. At 18.5 kV, the board broke down at Point

E in Figure 6(A). This seemed to verify that the offset cladding did indeed make the board more stable to high voltages, since the hole had appeared at a place where there was no offset.

While the breakdown phenomena was being observed, another large piece of printed circuit board was prepared. It had been determined, at least on this particular laser, that no traveling wave effect existed. Hence, the parabolic plate shape was really unnecessary and, in fact, removed a lot of useful board area. This design gave a much larger amount of plate area and a concurrent increase in the amount of stored energy. This modified laser board, therefore, did not have the parabolic shape as before, but instead, used a fully rectangular shape with the laser gap located at the center of the sheet so that the capacitor area was the same on both sides of the laser cavity. The spark gap hole was located in the corner, near the electrodes as shown in Figure 6(B). The edges were offset on the top to avoid the overlapping discontinuities.

When this board was fitted onto the laser cavity, there was no backup board available, so it was decided to use a relatively low voltage to avoid breakdown. Hence, the spark gap was set at 11.5 kV. It was quite surprising, then, to have the board break down after 3 hours of operation at this low voltage and a repetition rate of 3-4 Hz. The hole in the board occured at Point A of Figure 6(B). This

particular location is unusual in that it occurred on the spark gap side of the cavity, at a point where the board had been offset, when the voltage was relatively low (compared to the previous model board), and at a low repetition rate. This puncture was repaired with the same etch and fill method as described before. The spark gap was reduced further to 10 kV. The output power at this voltage setting was only 120 kW which was much lower than was desired.

A 60 ± 4 mil board had been received and it was etched in the same manner as that in Figure 6(B). In order to compensate for the increased thickness, and hence, lower available power, it was calculated that the input voltage must be increased from 11 kV to 16 kV. Since the maximum operating voltages of the thinner board appeared to be around 12 kV, it was estimated that the thicker board could easily accomodate at least 20 kV. Therefore, 16 kV did not seem unreasonable as a safe operating voltage.

When the 60 mil board was fired at this level for 15 minutes, it broke down dramatically. A large hole had been produced in the board at a point directly under the spark gap cover and the nylon retainer ring was punctured at three different locations. It was obvious that the limiting factor had become the spark gap assembly.

In order to increase the distances between conductors, a new spark gap was manufactured. The vertical distances

remained the same, but the horizontal dimensions were doubled in order to prevent further arcing and breakdowns and to reinforce the base material. This larger spark gap assembly operated normally but seemed to misfire more often. When this misfire occurred, the voltage would increase to 4 kV above the nominal level before the laser discharged. This occasional increase in the voltage required the use of even lower operating voltages, in order to insure the board safety. This, of course, reduced even further the output voltage of the pump laser. At voltages that were considered "safe", the output of the laser was considerably lower than previous designs. With the thick board in place, the laser could barely pump the two dye lasers simultaneously.

In summary, it could be deduced from the above factors that the thinner boards produced a greater amount of power at lower operating voltages. If a dielectric that could reliably withstand the necessary voltages could be obtained, the thin board would be considerably more efficient.

Several improvements are contemplated for this laser. The spark gap can be fitted with a standard spark plug which could be triggered by an external pulse generator. This would require a change in the electrical circuitry which would reduce the charging efficiency. Higher field potentials and repetition rates may cause problems in supplying enough fresh gas to the laser. The cavity box design allows room for a transverse flow arrangement. A series of

holes, drilled so as to point the gas stream into the active region, could be placed along one side of the box. A manifold would then be constructed along the side. Several gas exit ports on the opposite side of the box would serve to remove the hot gas.

The entire laser was very large and took up much laboratory space. The angled laser cavity also meant that the laser must be canted with respect to the region where the beam was being used. This further complicated the spacing of system components. It would be very beneficial to use a design which has its output emitted normal to the laser side. Since polarization is not considered crucial in the ultraviolet beam, the angled windows would be replaced by perpendicular windows and the entire box could be constructed in the form of an elongated rectangle. This would greatly facilitate construction of the cavity box and the electrodes.

Towards the end of this study, several new articles came to light which may provide the added needed powers. Kurnit et al [54] reported that, by using a xenon flashlamp and small quantities of a seed gas, they were able to eliminate the arcing and increase the laser tube pressures by employing photopreionization. If needed, the design of our laser cavity cover could easily accomodate the presence of the flashlamp. Additionally, Suchard et al [55] have announced a significant basic change in the nitrogen second positive band laser. By using a radically new discharge

tube (similar to the CO_2 TEA laser) and by adding SF_6, they have produced pulses with a risetime of 130 ns (3 times that of the lifetime of the C state) and pulsewidths of 480 ns. They speculate that the SF_6 depopulates the B state, thereby maintaining the inversion between C and B. Their powers were not disclosed, but they were not enough to lase a dye. With work, this type of laser could become significant in the future.

III. THE DYE LASER

F. P. Schäfer, in Dye Lasers [56], stated: "Dye lasers entered the scene at a time when several hundreds of laser-active materials had already been found. Yet they were not just another addition to the already long list of lasers. They were the fulfillment of an experimenter's pipe dream that was as old as the laser itself: To have a laser that was easily tunable over a wide range of frequencies or wavelengths." It is for this reason, that is, the dye laser's tunability, that this laser is particularly suited to Anti-Stokes Raman Spectroscopy. One dye laser can be tuned to a fixed frequency and a second dye laser can then be slowly tuned over a continuous range of frequencies, both with a high level of gain. The dye laser can do this easily. Semiconductor lasers have been developed that can be doped to perform at particular wavelengths (usually in the infrared), but the range is not continuous without an infinite number of laser junctions. Tunable Raman spin-flip lasers are tunable, but not easy to construct. The molecular structures of the organic chemicals are the basis for the dye laser's tunability and gain.

A. THE DYE LASER: THEORY

Organic dye molecules are characterized by one special feature: They are composed of a series of conjugated double

bonds — chains and rings of alternating single and double bonds (Figure 9). The pi bonding electrons exist in continuous clouds above and below the plane of the molecule itself. As the number of atoms in the molecule is increased, the number of electrons in the cloud increases and the electronic energy levels become more closely spaced. Superimposed on this electronic configuration are a large number of vibrational levels (from the large number of bonds present) which are themselves divided into a large number of rotational levels.

When one electron of a filled energy state is excited, it is promoted to a higher energy level (this transition usually occurs in the visible and ultraviolet). This electron can maintain its spin momentum resulting in a singlet state, or, less probably, undergo a spin flip to a triplet state. The combinations of these electronic, vibrational and rotational states produce an energy level diagram similar to Figure 10. Each of the electronic energy levels is composed of a continuum of vibrational and rotational levels.

In 1961, Rautian and Sobel'man [57] proposed a method of obtaining negative absorption (gain) from organic molecules. They realized that the ground to singlet state (S_1) transition (Figure 10) in organic molecules was the most effective. They proposed that if a molecule could be optically excited to the first singlet state, a small number of them would decay to the first triplet state (T_1). Since

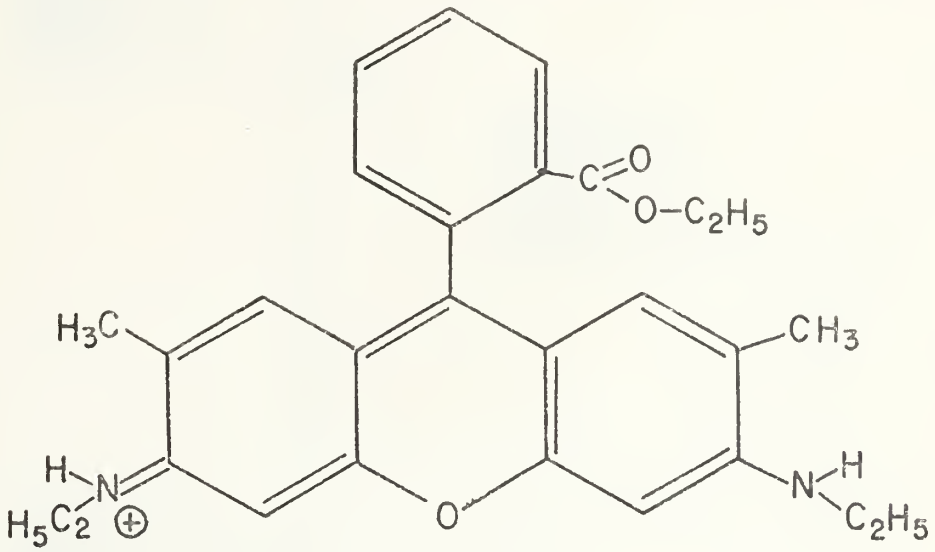

RHODAMINE 6G

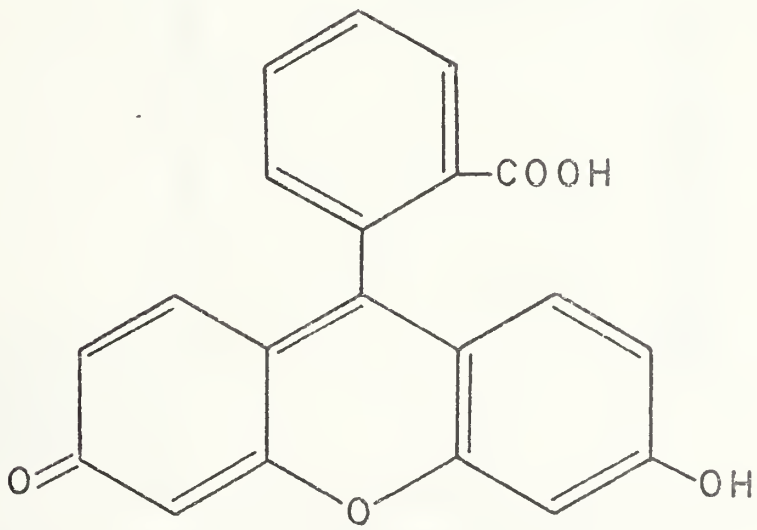

FLUORESCEIN

COMMON DYE STRUCTURES

FIGURE 9

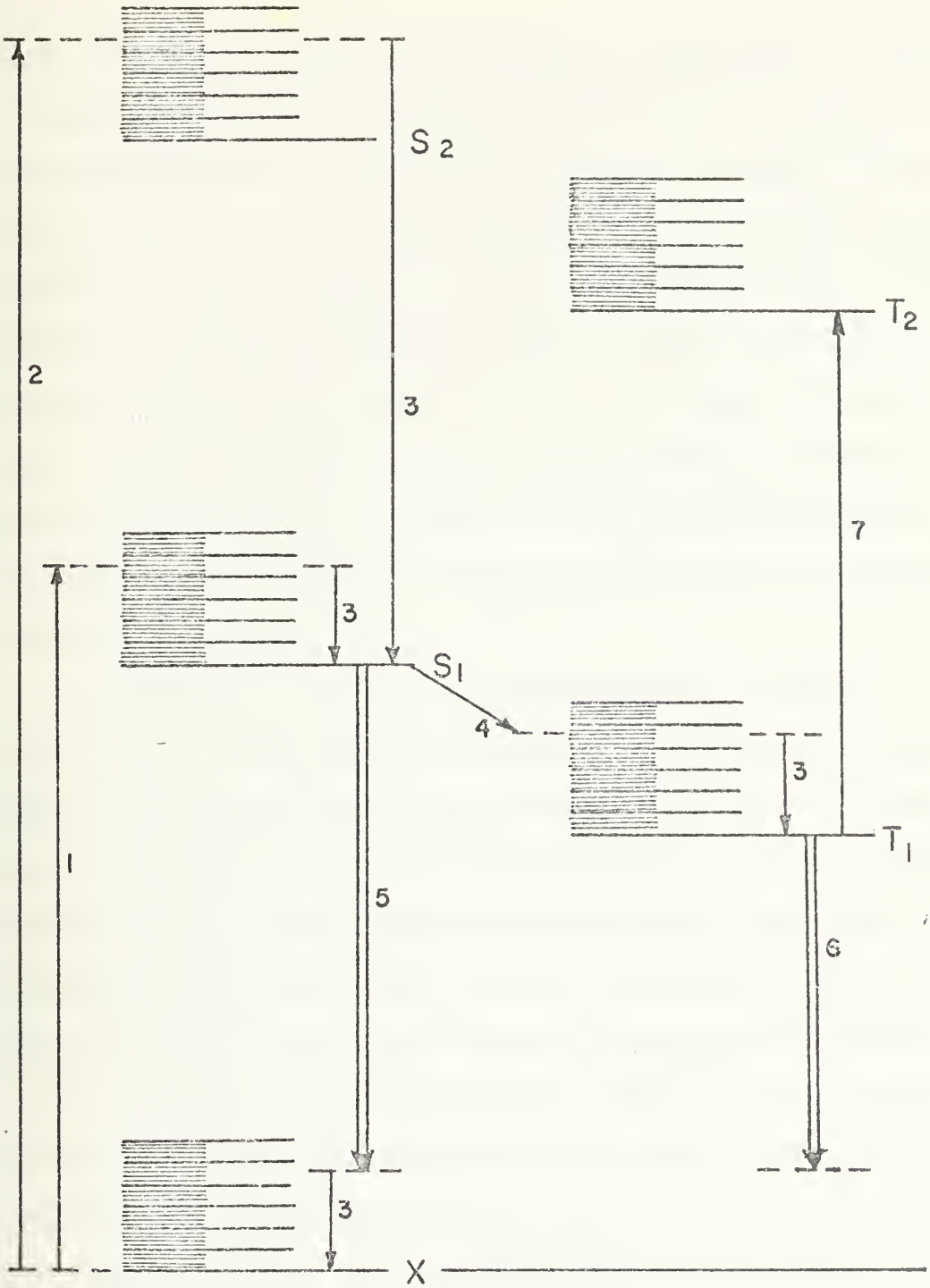

ENERGY LEVEL DIAGRAM OF A DYE

FIGURE 10

this triplet to ground transition is forbidden, a number of molecules would accumulate in the triplet state. In the ground state, only the first few vibrational levels are filled due to Boltzmann statistics, so that the upper levels are not occupied. All of this could result in an inversion between the lowest lying triplet level and the higher levels of the ground state. This was a phosphorescent laser. They were certainly thinking in the right direction, but, as it turns out, the entire process is negligible compared to a singlet to singlet, or fluorescent, laser.

Stockman et al [58], in 1964, analyzed these two types of lasers. They used the standard equation for the determination of population difference densities and discovered that it would require a concentration of 10^{20} molecules/cm^3 and exceedingly high pump powers to reach threshold. They recognized that even this did not guarantee lasing as there were sure to be triplet-triplet absorptions that would further hinder the phosphorescent laser. The team did, however, correctly predict that a singlet to singlet fluorescent laser would be feasible. The required pump powers and concentrations were acceptable and the relaxation times were appropriate for establishing a population inversion. They attempted to achieve lasing from a dye laser, but failed because of their choice of dyes [56].

The actual dynamics of dye population inversion is as follows. An optical pump can place molecules in the first excited singlet state, S_1, by either of two methods. At longer wavelengths, the molecule absorbs energy and is lifted directly to some appropriate level in S_1 (process 1). The molecule rapidly goes through radiationless internal conversion (process 3) to the lowest vibrational level of S_1. If the exciting radiation has a shorter wavelength, the molecule may be excited directly to some level in the second excited singlet state, S_2 (process 2). The lifetime of S_2 is very short ($\tau = 10^{-12}$ sec.) and it undergoes a rapid, radiationless internal conversion (process 3) to the lowest lying vibrational level of S_1. Hence, by one form or another, all of the transitions have ended up at the lowest level of S_1. There are therefore a significant number of molecules at this level. In the ground state, X, most of the molecules have remained in the lowest levels (from Boltzmann statistics). There is now an inversion between the lowest level of S_1 and any of the upper (unoccupied) levels of X. The molecules may then undergo spontaneous or stimulated emission (process 5) to any or all of the empty levels in the ground state. Since there are almost an infinite number of empty levels in X, the fluorescence wavelength is a continuous band determined by the energy difference between S_1 and the various empty levels. When a molecule decays to a level in X, it undergoes a

transition to the lowest levels, maintaining the population inversion.

There is a competing process, however. If the molecule remains in S_1 for a time longer than its lifetime ($\tau = 10^{-8}$ sec.), it can undergo intersystem crossing (process 4) to the lowest lying triplet state, T_1. From here, it can behave in two ways. It can return to the ground state, a forbidden triplet to singlet transition ($\tau = 10^{-4}$ to 10^{1} sec.), or it can be excited to a higher triplet state. The latter is more likely as it does not involve a spin momentum change. The decay from S_1 to T_1 is an undesirable effect in current lasers for two reasons. Any molecules that are taken out of S_1 reduce the number that can undergo stimulated emission. Furthermore, once the molecule is in T_1, it can readily absorb light and go to T_2. This action depletes the amount of light that can be used to stimulate molecules from X to S_1.

If the pulsewidth of the optical pump is greater than 10^{-8} sec., a significant number of molecules can accumulate in the triplet state and completely quench the lasing action. For pump lasers such as the nitrogen, giant pulse ruby or neodymium lasers, this intersystem crossing effect is of little concern. For long pulse or cw pumps, however, it may completely stop the laser. Workers have been able to get around this problem in several ways. If the dye is flowed rapidly through the pump beam, fresh molecules in X are

continually excited and lasing proceeds. There is no time to build up an appreciable number of molecules in T_1. A triplet state quencher can also be added to the dye solution. These molecules physically interact with the dye molecules in T_1. Those in T_1 transfer their energy directly to the quencher and return to the ground state.

If normal processes occur, the absorption and emission spectra take on the appearance of Figure 11. As would be expected from energy conservation, the absorption band is located at lower wavelengths than the emission spectra. The knowledge of the emission-absorption spectra of each dye used can be invaluable when optimizing the absorption of pump radiation. Ultraviolet light may be only weakly absorbed by dyes which emit in the red. It may then become possible to add a secondary dye to the laser solution which absorbs the uv light and radiates in the region of maximum absorption of the primary dye. Such an absorption-emission-absorption-lase mechanism is called selective energy transfer and may increase the efficiency of a particular pump-dye combination by a factor of 10.

As shown in Figure 11, the dye laser can radiate at any wavelength under the emission curve that is above the threshold limit (indicated by the dotted line). Such laser emission can have a very wide bandwidth. Some dyes, which have extremely high gains, can exhibit an effect known as superradiance. The pumped region radiates coherently along

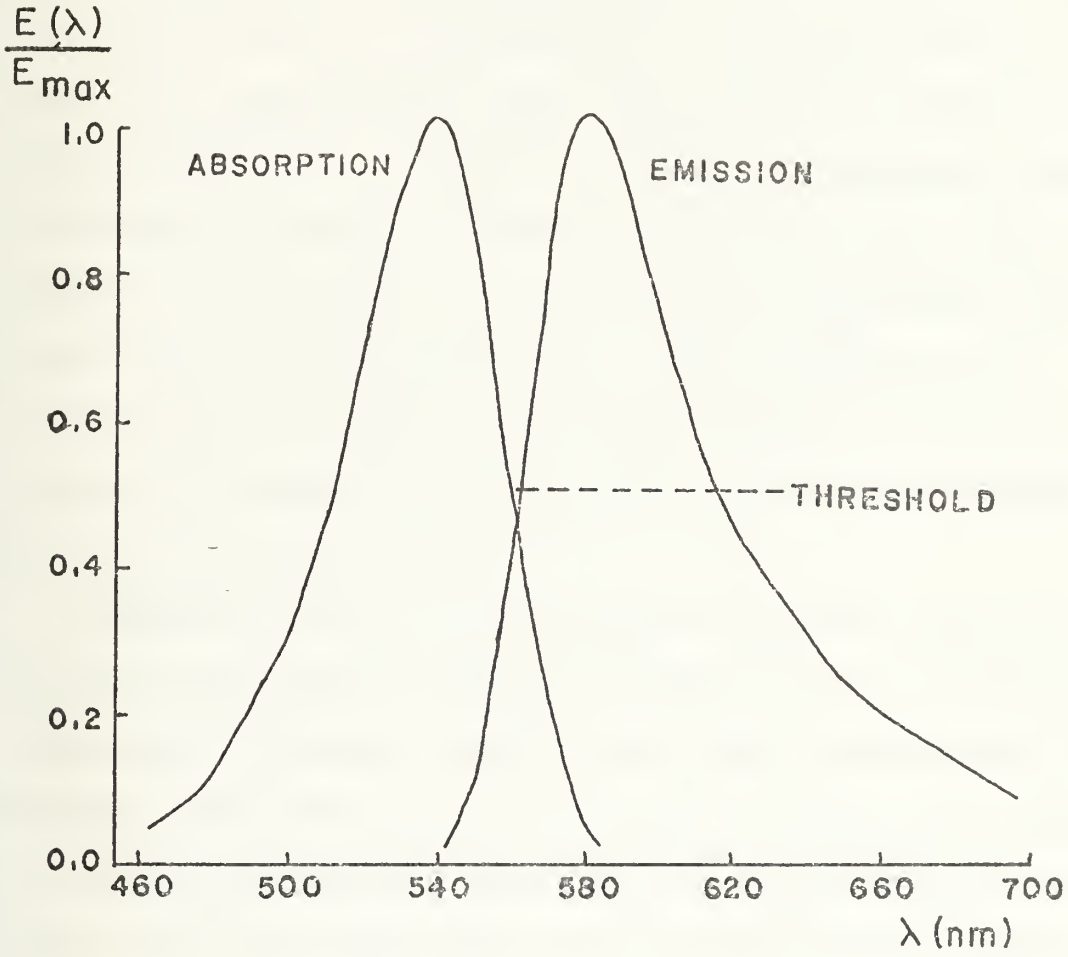

SPECTROPHOTOMETRIC DATA FOR
RHODAMINE 6G (SCHÄFER)

FIGURE 11

its line of maximum gain, doing so without a resonant cavity. The output is collimated but has a higher divergence angle than the output from a laser with mirrors. Super-radiant emission is very broad-band and is often undesirable. It can be reduced or eliminated by defocusing the pump beam. For spectroscopic work, any broadband emission is highly undesirable. In order to obtain narrowband emission, it becomes necessary to introduce into the laser cavity an element that has low loss at the desired wavelength and high loss at other wavelengths. This function can be accomplished by spectral absorbers (bandpass filters) or dispersive elements, such as prisms, gratings or etalons, or combinations of these.

Bandpass filters are not often used since they are designed for specific frequencies and will not provide for continuous selection. On the other hand, etalons are very sensitive and are usually used in conjunction with prisms or gratings in order to provide greater narrowing of the light coming off the latter two devices [59-62]. Recently, mirrorless distributed feedback tuning has been reported [63,64].

Both gratings and prisms are used in modern tunable dye lasers [65-72]. Both are lossy at all wavelengths, but much more so at untuned frequencies. Prisms must be specially constructed so that light enters and leaves at Brewster's angle and they should also have non-reflective

coatings. In order to provide for the maximum dispersive effect, the mirror (Figure 12(A)) should be as far from the prism as possible. This leads to a large, often cumbersome setup but has the advantage of being very selective. Some lasers have been constructed with as many as six prisms in a continuous circle. Prisms are often used where very high power (usually cw) beams are involved. Since the light passes through them unattenuated, they tend to resist heating effects and damage better than other tuning devices.

Gratings are often used because they are available for nearly all wavelengths, are easily aligned and tuned and result in a compact laser cavity. Hard [73] has analyzed modern gratings and has determined that, while they are widely used and relatively efficient, there is much room for improvement, mainly in the development of more optimum groove shapes. The grating is inserted into the laser cavity as shown in Figure 12(B). When the laser beam strikes the grating, there are two beams reflected from it at an angle on each side of the normal. They are identical except that one is considerably more intense. It is this intense beam that is fed back into the laser cavity. The light that comes off in the weaker beam is usually lost. Most dye lasers have the grating mounted in Littrow, which means the reflected beam follows the same path as the incoming beam. Other configurations use the light coming out the side of the laser as the output. Here, the front mirror is a total

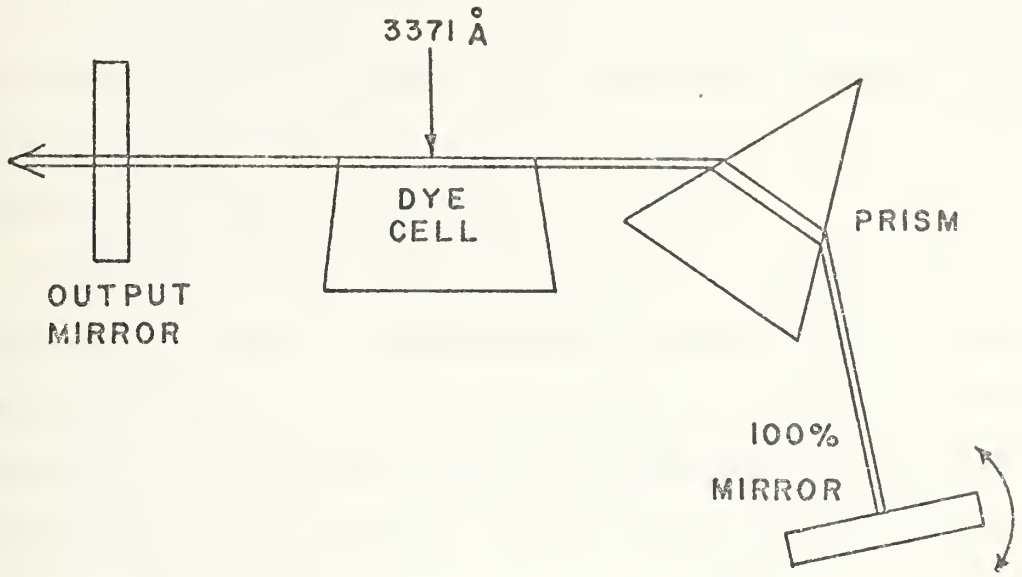

(A) PRISM

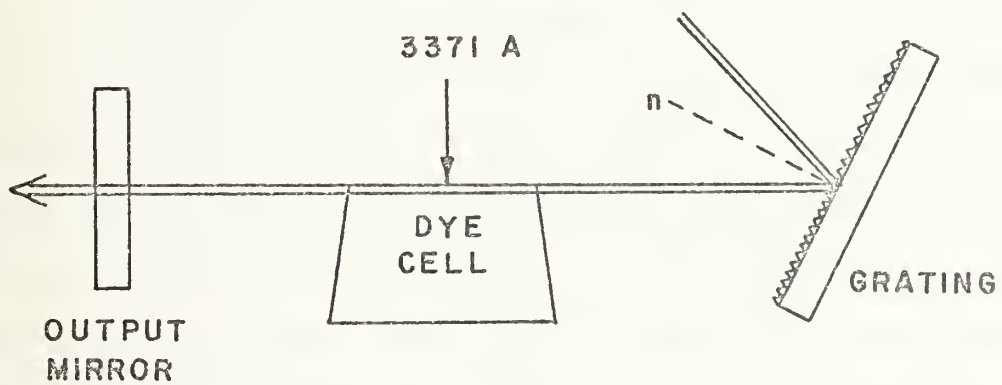

(B) GRATING

DYE LASER CONFIGURATIONS

FIGURE 12

reflector. Hard has also determined that the groove spacing on the grating should be between 0.5 and 1.5 times the wavelength of the light. This allows for tuning, but means that separate gratings must be used for various major portions of the electromagnetic spectrum.

Hänsch [74] has described a pulsed tunable dye laser that can be used for spectroscopic purposes. His basic setup is shown in Figure 13. This has become the standard design for pulsed dye lasers. Hänsch has inserted an expanding telescope between the dye cell and the grating. The resolution of a grating is dependent on the amount of grating area illuminated. He also has inserted an etalon in front of the grating to further reduce the bandwidth.

To complete the resonant cavity, a mirror is mounted at the front end of the dye cell. This mirror usually has a transmission of 30 to 50%. This is quite lossy for a laser. Since this is a pulsed laser and the pulses are very short, there is only time for a few passes through the laser. Hence, the pulsed dye laser is treated as a semi-superradiant laser. Only half of the radiation coming out the front of the dye cell is fed back into the laser. This is usually weak compared to the radiation that is emitted from the back of the cell, strikes the grating (and reduced to a narrow frequency range), and is then fed back into the dye cell, stimulating a considerable amount of light at the specific frequency. The overall output of the laser

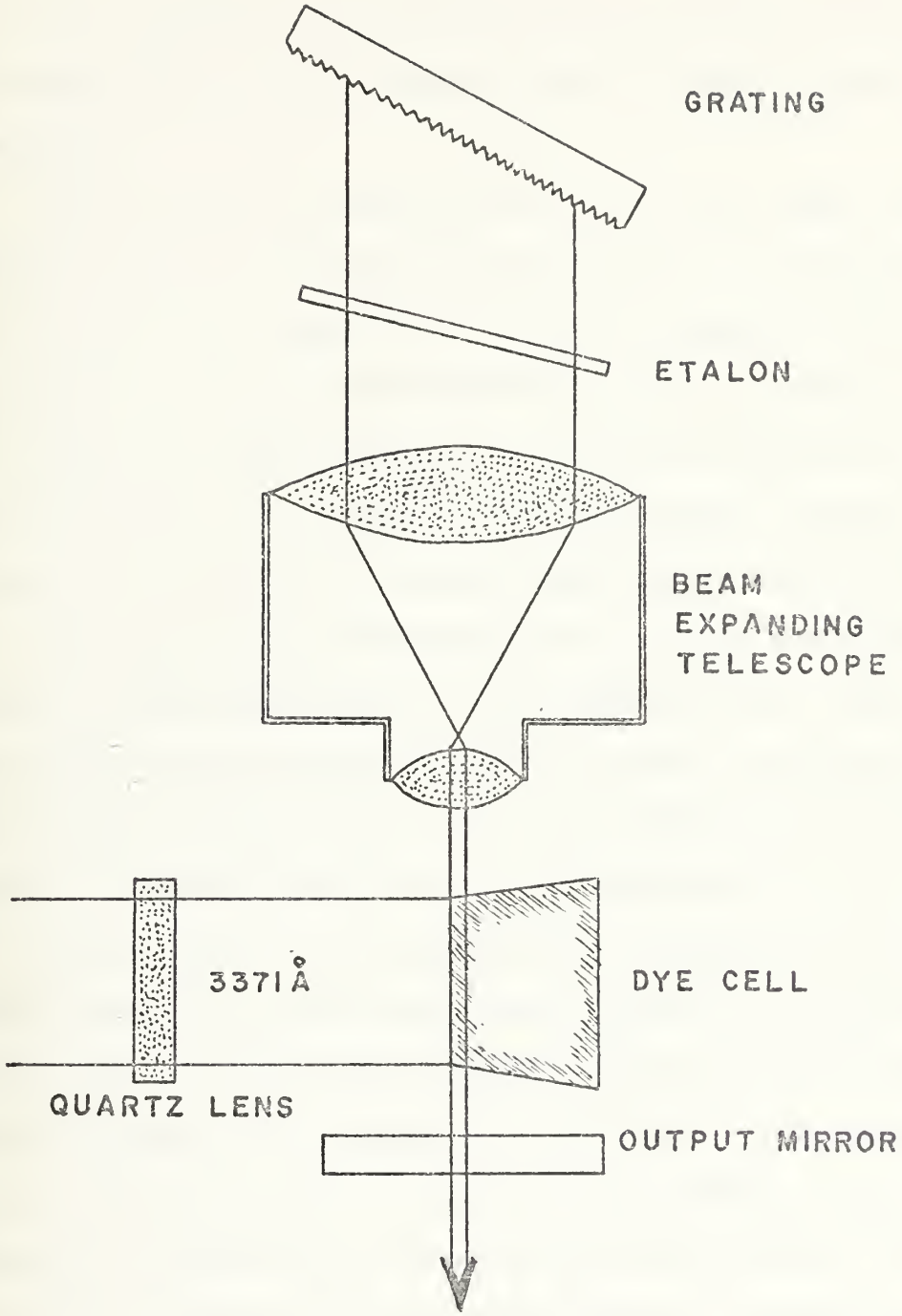

PULSED DYE LASER

(HÄNSCH)

FIGURE 13

is a weak broad band of superradiant radiation upon which is superimposed a very strong spike of light at the tuned frequency.

The dye cell is constructed so that its faces are not perpendicular to the laser beam direction. This prevents the dye cell from becoming a laser in itself. The reflectivities of the cell ends effectively act as mirrors and the internal lasing severely degrades the effect of the tuning element. To complete the apparatus, a quartz lens is used to focus the nitrogen laser beam into the cell.

The laser shown in Figure 13 is typical for transversely pumped dye lasers. The configurations used in cw or longitudinally pumped lasers are quite different and will not be investigated here. The main differences are the types of mirrors used and cavity geometries.

The dye laser is, in principle, a simple, efficient device which has many useful applications. As with any laser, the component parts must be of very high quality and exact alignment is manditory if the laser is to operate to its fullest extent. These two requirements pose the greatest problems when constructing a dye laser. The parts used must be built to the finest optical tolerances and the cavity components must be extremely stable. The optical parts and their holders are easily the most expensive part of the laser. With the proper parts and time, an efficient, tunable laser source can be constructed.

B. THE DYE LASER: EXPERIMENTAL

When a 3371 Å source had been developed which was believed to be capable of pumping a dye laser, it was decided to attempt to achieve lasing action using the most basic and efficient dye laser system. Rhodamine 6G (Figure 9) was the obvious choice for the laser medium. It has the highest gain and one of the widest lasing wavelength regions of any dye currently in use.

Absolute ethanol was used as the solvent. Many solvents (water, DMSO, methanol) can be used but ethanol has been shown to exhibit the best combination of tuning range, solvency and gain of those used. The absorption (transmission) spectra of Rhodamine 6G, Rhodamine B and Brilliant Sulfaflavavine were obtained using a Beckman DB Spectrometer. At low concentrations, it appears that the efficiency of absorption in the ultraviolet is low (Figure 14). Note that Rhodamine B, which fluoresces at longer wavelengths than Rhodamine 6G, also absorbs at longer wavelengths. The small rises in the Rhodamines in the ultraviolet may be due to direct transitions to the second excited singlet state. As the concentrations are increased, the absorption becomes almost 100% across the entire region of interest. This is especially true for Rhodamine 6G at concentrations which are normally used in transverse uv pumping arrangements. (3371 Å is indicated in Figure 14 by the arrow.)

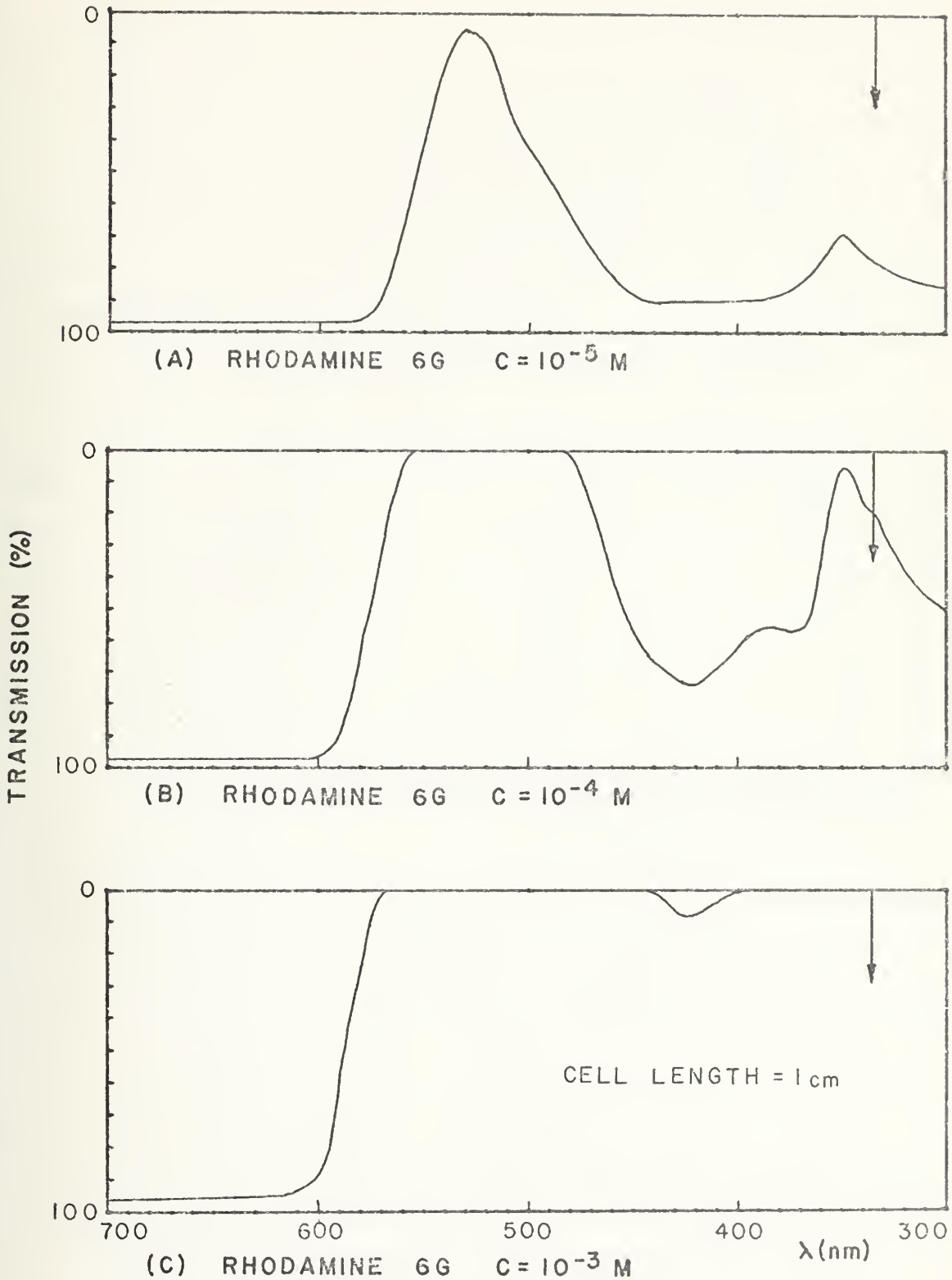

ABSORPTION SPECTRA

FIGURE 14

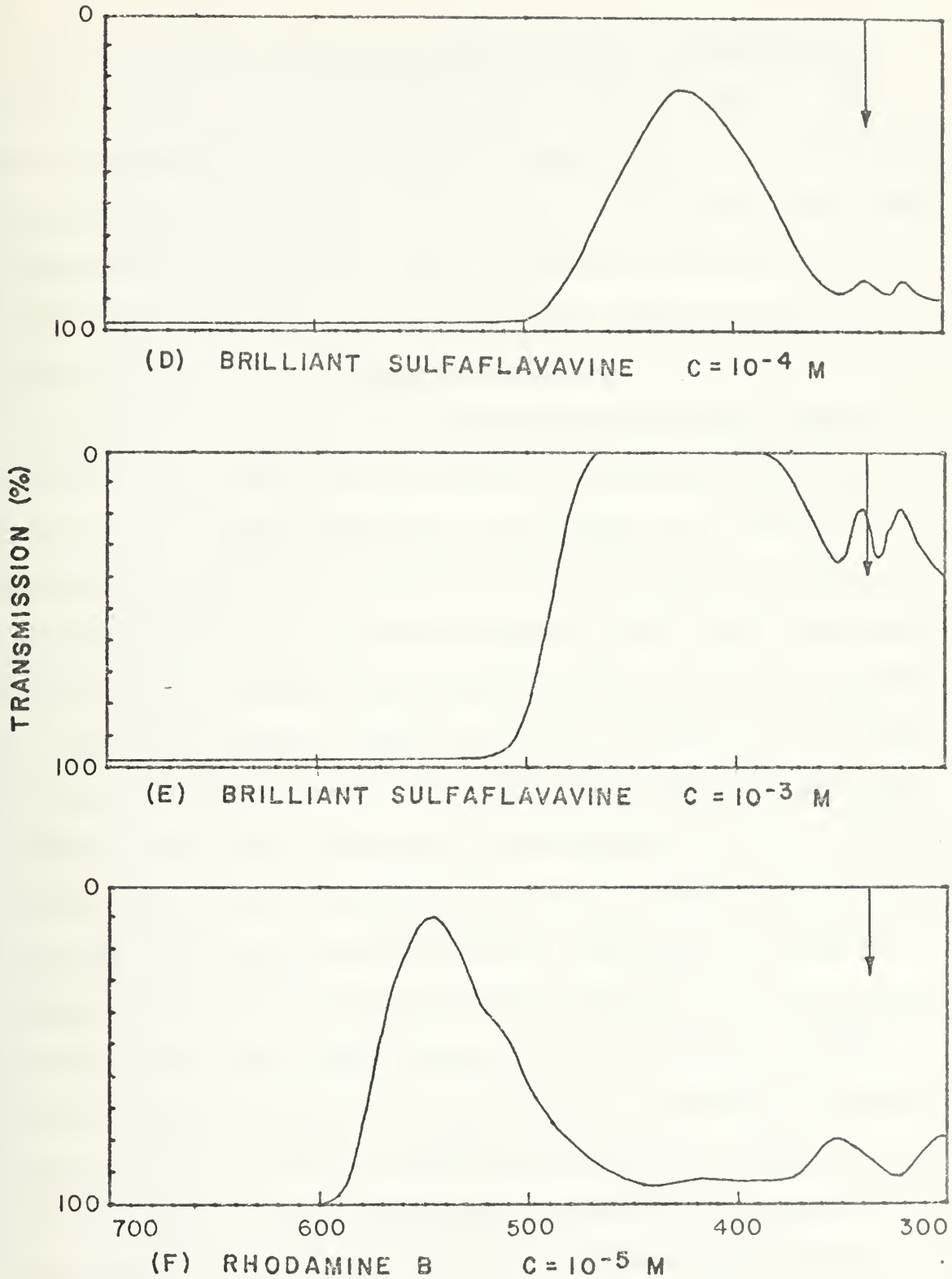

ABSORPTION SPECTRA
FIGURE 14 (CONT)

A cylindrical, parallel-end dye cell, 20 mm long by 20 mm diameter, was originally used (Figure 16(A)). It was commercially available in uv grade quartz. At that time, the deleterious effects of the parallel ends were not known. It was also later learned that the curved surface of the cell tends to defocus the uv beam and, hence, partially defeats the effect of the focusing lens.

The resonant cavity was constructed from two concave mirrors, each with a focal length of 27 cm, and separated by 27 cm. The total reflector was coated with aluminum and had a reflectivity of 100%. The output mirror had an aluminum coating and a reflectance of 98%. This combination was used to make the cavity confocal and to have the maximum Q. Since the Schenck laser would not, at that point, raise the dye to superradiance, this radiation could not be used to align the cavity (this will be discussed later). Therefore, a HeNe laser was aimed through the output mirror and the resulting multiple reflections were used to align the system. During this procedure, the effects of the parallel dye cell ends were first noted. It was decided, wrongly, to alleviate the spurious reflections by carefully aligning the dye cell so that any reflections would be fed back along the beam path. Lasing was finally obtained by adjusting the mirrors until the first signs of stimulated emission was observed. The resultant yellow-orange laser beam was very weak but could be observed striking the wall across

the darkened room. The beam divergence was on the order of 2 mrad.

Discussions with Dr. J. Trias* indicated that most pumps of useful powers should be able to stimulate the Rhodamine 6G to superradiance. He also noted that the concentration of the dye solution (10^{-3} M) was in the right range for this type of laser, but that it should be adjusted so that the absorption region extended into the dye cell the same distance as the height of the absorption region — approximating a square active region.

At this time, the Nagata laser came back into use and it was decided to return to it in hopes of obtaining more power. The following procedure has been used to align all of the beams involved in the dye laser system. The nitrogen laser was turned on and its beam was observed with a fluorescent plate. The quartz cylindrical lens was then placed in a position so as to collect the area of greatest intensity. The dye cell was placed in the focused beam and adjusted to a position where the beam appears to be optimally focused. It was at that point that superradiance was first observed when using the Nagata laser as the pump. A collimated beam was emitted from the dye cell without the use of

---

*Dr. J. Trias, of the Naval Electronics Laboratory, San Diego, has provided very generous amounts of his time analyzing problems encountered and recommending solutions.

any of the mirrors that comprise the optical cavity. This beam had a divergence of 4-5 mrad. The presence of this superradiance greatly facilitates the alignment of the remainder of the system. The output mirror was placed at one end of the dye cell and the reflection noted on a sheet of paper at the other end of the dye cell. The mirror was then adjusted until the reflection from the mirror overlapped the superradiance. With slight additional tuning, the output on the paper suddenly increased in intensity. The total reflector was then placed at the other end of the dye cell and a piece of paper was placed where the beam emerges from the output mirror. The 100% mirror was then adjusted until a relatively strong laser beam emerged from the output mirror.

Several features were noted in the laser cavity. The most troublesome was the inability of the mirrors to compensate for the beam divergence and to focus the rays tightly back into the dye cell. Various mirrors, with different radii of curvature, were tried with only limited success. A partial solution will be described later. In addition, the output mirror had such a large relectivity that only a small portion was coupled out of the cavity. Therefore, a series of mirrors, with reflectivities ranging from 50 to 85%, was tried in the system. As the transmissivity of the mirror increased, the output intensity increased, but the beam degraded somewhat and it appeared

that much of the radiation was coming directly from the dye cell, and that very little was the result of multiple oscillations.

A grating, obtained from PTR Optics, was then mounted in the laser, in place of the total reflector. This grating was especially designed for use in dye lasers, and was etched for maximum dispersion at 5000 Å. It was suitable for use throughout the visible region, however. Since the laser was to be tuned by rotating the grating about a vertical axis, the rulings of the grating must also be positioned vertically. If the grating is slightly off-axis, the beam coming off the grating will not smoothly scan the dye cell and numerous adjustments will have to be made to the grating alignment as the grating is rotated. A particularly simple method was discovered for obtaining this correct vertical alignment. The superradiant output of the dye cell was used to illuminate the grating at an angle normal to it. Two beams were reflected off the grating, at an angle on each side of the normal. The grating was then rotated in the holder until the two beams emerged in a plane that was parallel to the table. Since this plane was normal to the grating rulings, the rulings were normal to the table, and were, hence, vertical. One of the two beams which emerged from the grating was much more intense than the other. It was this intense reflection which was fed back into the dye cell.

A problem, similar to the one encountered with the output mirror, was noted. The beam, by the time it hit the grating and returned to the dye cell, had diverged to such a large area that there was only a slight tuning effect which could be seen mixed with a considerable amount of superradiance. Two remedial steps were taken to solve this problem. An extension was mounted on the output mirror holder so that the mirror was placed in close proximity to the dye cell. The beam traveled only about 4 mm as it went from the dye cell to the mirror and back to the cell. This short distance prevented any appreciable spreading and improved the beam quality considerably. At the grating end of the cell, an optical beam expander, purchased from Oriel, was installed between the dye cell and the grating. As the beam emerged from the dye cell, it was expanded to ten times its original size. This enabled more of the grating to be used and hence reduced the bandwidth of the desired frequency. Since the beam expander is mounted in Littrow, the light coming off the grating is focused to a very tight beam which is then coupled back into the dye. These two improvements, taken together, vastly improved the beam power and quality and considerably narrowed the spectral output.

The entire arrangement, as described above and shown in Figure 13, was applied to the Godard laser. A variety of dyes were then tried in the laser. The output was

observed with a 1 m Jarrell-Ash Ebert Grating Spectrometer. The results are shown in Figure 15 and described in Table II. The only dye (in our possession) that would not lase was the Di-Butoxy-POPOP that was obtained from NWC, China Lake. The solubility of the compound was limited and suitable concentrations could not be attained. Later, Toluene was used as the solvent. A higher concentration was achieved and the dye lased weakly in the deep blue region. As can be seen from Figure 15, a large portion of the visible spectrum is covered by the dyes listed. The relative intensities of some of the dyes limit their usefulness in studies requiring high powers, but they do provide coherent radiation over a wide range of frequencies that could be used for some forms of spectroscopy and remote monitoring. (The curves in Figure 15 are approximated by parabolas – which are, in fact, close fits to the observed curves.) A more complete list of dyes is presented in Reference 56 (p. 180-193) and References [75-81].

Although reasonable outputs were now being obtained, the problem of the mini-lasing between the parallel ends of the dye cell remained. The multiple reflections from the grating, mirror and two cell ends resulted in a multimode output that was unacceptable for the focusing and beam mixing that was required in CARS. A modified cylindrical dye cell was tried in the laser. It was constructed out of pyrex tubing with a 15 mm diameter. Flat microscope slides were carefully cemented to the ends at 10° off the

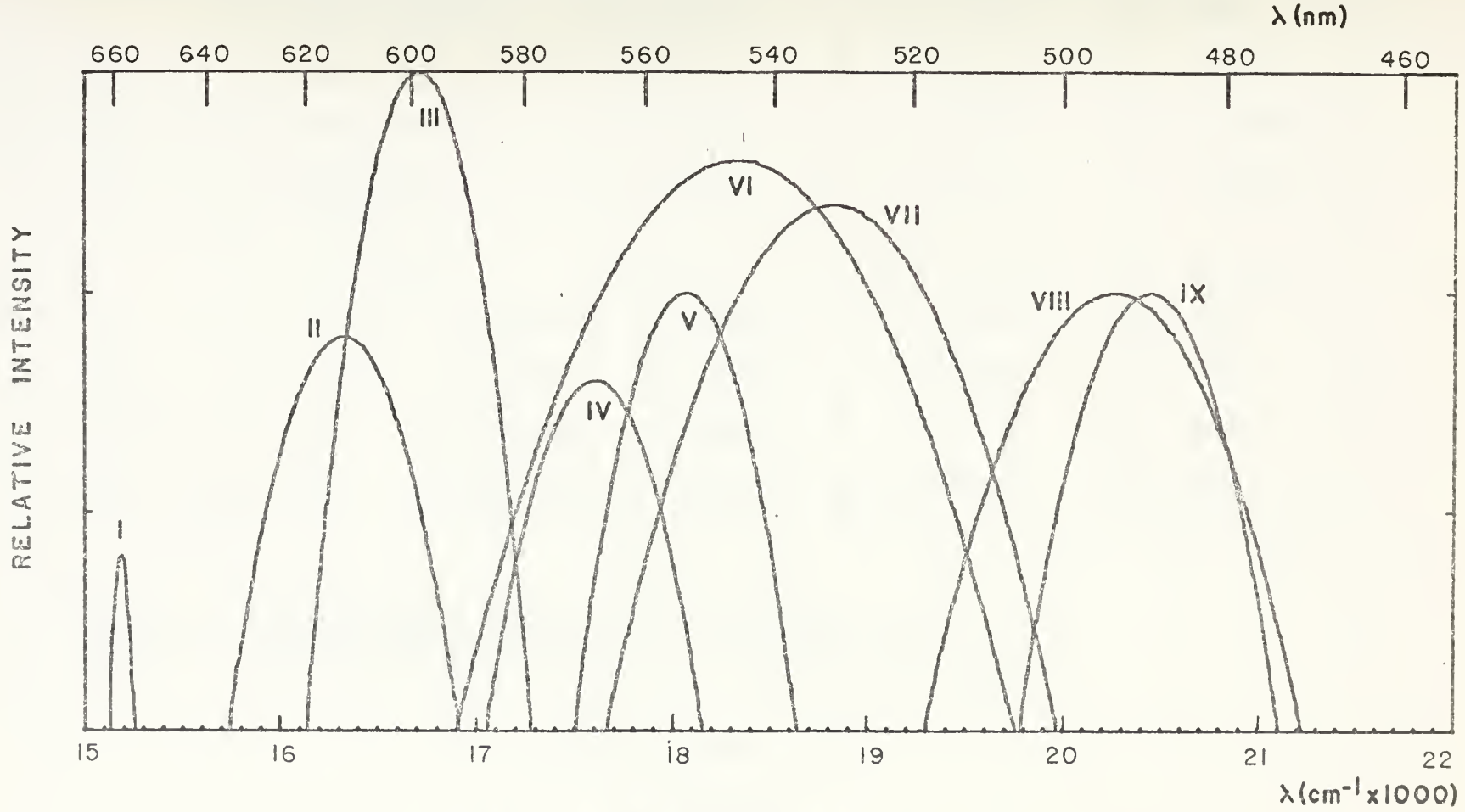

DYE LASING CURVES

FIGURE 15

FIGURE 15 CODE	DYE	SOLVENT	WAVELENGTH RANGE (nm)	SOURCE[1]
I	Cresyl Violet	Ethanol	661-655	NWC
II	Rhodamine B	Ethanol	635-591	Eastman
III	Rhodamine 6G	Ethanol	620-578	Eastman
IV	Dichloro-Fluorescein	Ethanol	583-551	Eastman
V	Fluorescein	Ethanol	571-536	Eastman
VI	ANC-NMe (Coumarin)	p-Dioxane	592-506	NWC
VII	ANC-NH (Coumarin)	p-Dioxane	566-500	NWC
VIII	ClF (Coumarin)	p-Dioxane	518-471	NELC
IX	ANC (Coumarin)	p-Dioxane	506-475	NWC

[1] NWC Naval Weapons Center, China Lake, CA
Eastman Eastman Kodak Chemical Co., Rochester, NY
NELC Naval Electronics Laboratory Center, San Diego, CA

OBSERVED LASER DYES

TABLE II

normal. Figure 16(B) shows this design. It was difficult to properly construct this cell and, because of the angled faces, the beam was refracted as it emerged from the cell. This refracted beam made the laser more difficult to align and the geometry required did not allow the cavity length to be minimized.

During a trip to Stanford University, T. W. Hänsch's cell design was observed and it was duplicated in our laboratory. This design is shown in Figure 16(C). The cell had a path length of 10 mm and was ideal for small cavities. It could be tilted until multiple reflections from the cell ends disappeared. It could also be modified to allow the dye to be pumped through the cell. This, it was reported by Hänsch's group, was necessary when large pump powers were employed. Since the volume of the cell was small, there was little room for mixing and decomposed dye molecules soon accumulated. Not only did the output power decrease, but also the molecules were burned onto the cell window faces.

One final solution used was to elevate one end of the cylindrical dye cell in its holder until the multiple reflections ceased and then to insert a spacer under the cell end to maintain this orientation. This final design was used more often than the others because it was larger and allowed the full 20 mm of the dye to be pumped. This was necessary to obtain the powers necessary for the CARS

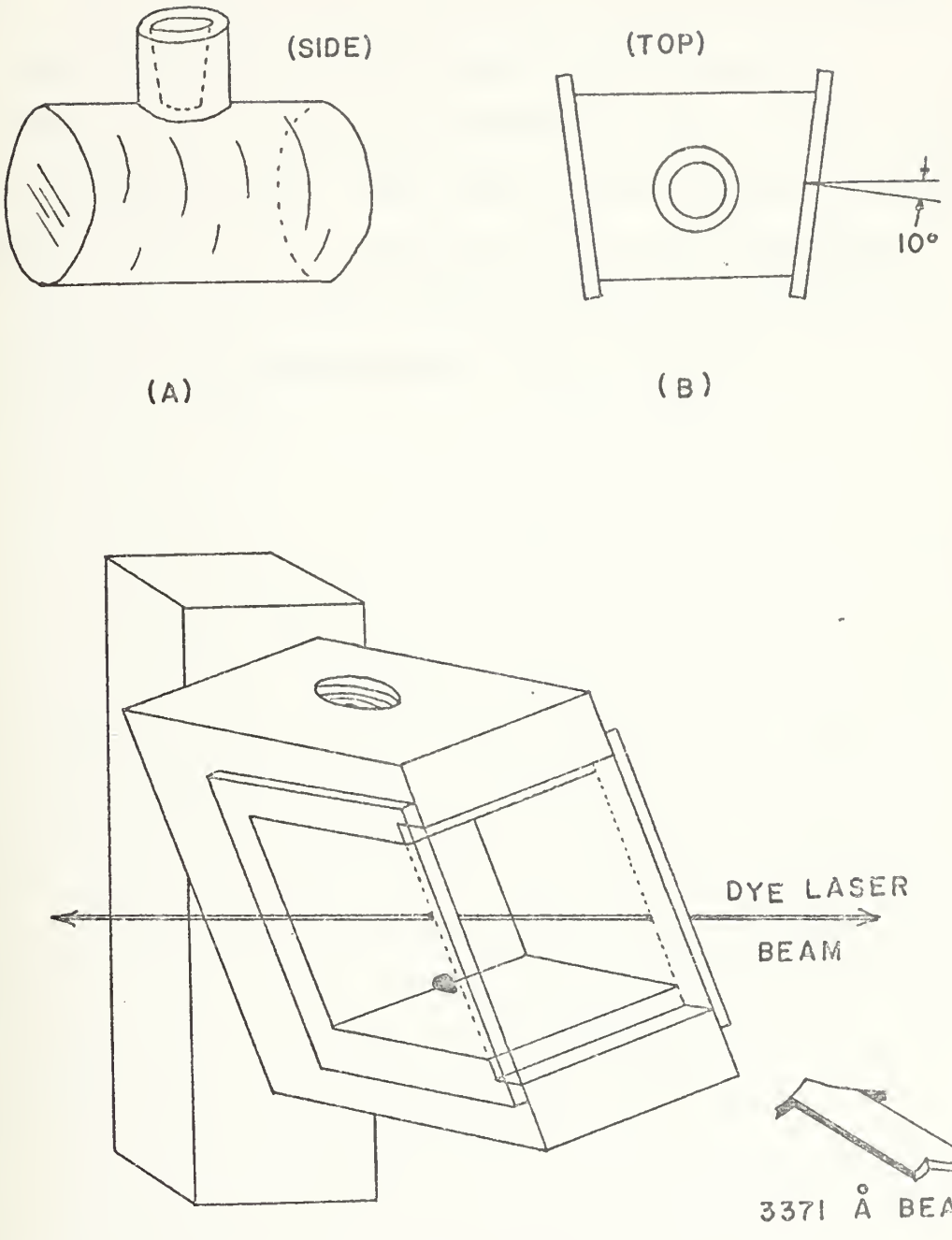

DYE CELL DESIGNS

FIGURE 16

effect. In addition, the large volume of the cylindrical cell made the use of flowing apparatus unnecessary.

Since tunable lasers are needed for CARS, two dye lasers had to be constructed. Both used the basic design reported by Hänsch (Figure 13). Since no etalons were available, they were not used. The bandwidth observed in Rhodamine 6G at 5000 Å was approximately 3 Å or 12 cm^{-1}.

IV. COHERENT ANTI STOKES RAMAN SPECTROSCOPY

In 1965, Terhune and Maker [82] revealed that they had observed both coherent Stokes and coherent anti-Stokes Raman radiation when they focused a high intensity laser beam into a Raman active material. The outputs were limited to conical sections which were much more intense than the standard Raman radiation. Their experiments demonstrated that the nonlinear effects of materials could be studied by using high intensity beams that would make these, otherwise weak, higher order (interaction) outputs easier to measure and analyze. At first, most workers in the field concentrated on the second order effects and the Stokes radiation. Since a fully tunable laser had not been developed at that point, the anti-Stokes side could not be selectively pumped. Therefore, the samples were analyzed with fixed frequency lasers and the more powerful output beam (Stokes) was singled out and analyzed, even though there were often background fluorescence problems.

It was later noted that other orders were being produced by the interactions of the pump beam and first order Raman beam. Hence, the two wave mixing effect was first observed. During the middle and late 1960s, many articles reported the analyses of various types of materials (liquids, crystals, semiconductors) using stimulated Raman techniques. These second order studies soon gave way to even higher order

experiments, wherein three, or more, beams of various frequencies were mixed to get various sum and difference interactions.

Although three wave mixing work was being pursued as early as 1972, it merely took advantage of the Raman resonances without applying it directly to Raman studies. In 1974, several articles appeared reporting the use of Coherent Anti-Stokes mixing, or four wave mixing, to determine the Raman spectra of various materials. All of these used tunable dye lasers to induce the non-linear interaction and beam production in the sample being studied. A fixed dye, or pump, laser was used to produce two quanta at the Raman pump frequency and a dye laser produced one quanta at the Stokes frequency. The three waves were mixed, via the nonlinear Raman material, to produce a fourth quantum at the anti-Stokes frequency. This latter beam was at a higher frequency than the natural fluorescence, was collimated and had a reasonably high conversion efficiency.

The CARS concept requires an understanding of the Raman effect (the final application) and of the non-linear properties of materials which enables the method to reproduce the Raman spectra. These are presented in the following sections. The experimental results are reported in the final section.

A. COHERENT ANTI STOKES RAMAN SPECTROSCOPY: THEORY

1. The Raman Effect

In the 1920s, while analyzing the scattering of light by liquids, C. V. Raman observed not only the expected unshifted Rayleigh scattering but also a modified pattern that was shifted in frequency from that of the fundamental light. When he used a mercury arc lamp, he found that "...each line of the incident radiation, provided it was of sufficient intensity, gave rise to its own modified scattering, and the frequency shifts, the relative intensities, the state of polarization, and other features of the new lines and bands were independent of the exciting radiation." [83] In fact, he found that these shifts were dependent on the material that was being analyzed. He also saw these shifted lines on each side of the fundamental frequency. The light that emerged from the sample that had a lower frequency was eventually called the Stokes radiation while that radiation on the other side, with up-shifted frequency (and hence greater energy than the fundamental), was called the anti-Stokes radiation. The intensities of the Stokes lines were much higher than the anti-Stokes lines.

The importance of this Raman effect became more pronounced when it was determined that the energy differences involved in the shifting of the light was on the order of the vibrational energy differences of the molecule being studied. This interaction between the photon of light and

the molecule is often represented by a diagram such as Figure 17.

When photons, with frequency ν_{in}, strike a group of molecules, they impart an energy, equal to $h\nu_{in}$ to some of the molecules. Since these molecules are at room temperature, the population of the vibrational levels is initially determined by the Boltzmann factor. During the scattering process, some of the molecules originally in the ground state are excited to a higher vibrational level. During this process, the incoming frequency is shifted to a lower (Stokes) frequency, with the photon energy difference equal to the vibrational energy. In this process, some molecules in a higher vibrational level impart a unit of energy to the incoming wave as they scatter to the ground state. The scattered light is upshifted in frequency (anti-Stokes) from the incoming light. As can be seen, the Stokes photon energy is less than the fundamental photon energy by the amount ΔE_v while the anti-Stokes photon is greater by ΔE_v. Here, ΔE_v is the difference in energy between the vibrational energy levels. It also develops that the rotational energy levels can be analyzed in the same basic form but, of course, the energy level differences are much smaller and require more precise equipment to distinguish the frequency differences.

The above discussion is based on the fact that there are virtual levels available to be used as the intermediate

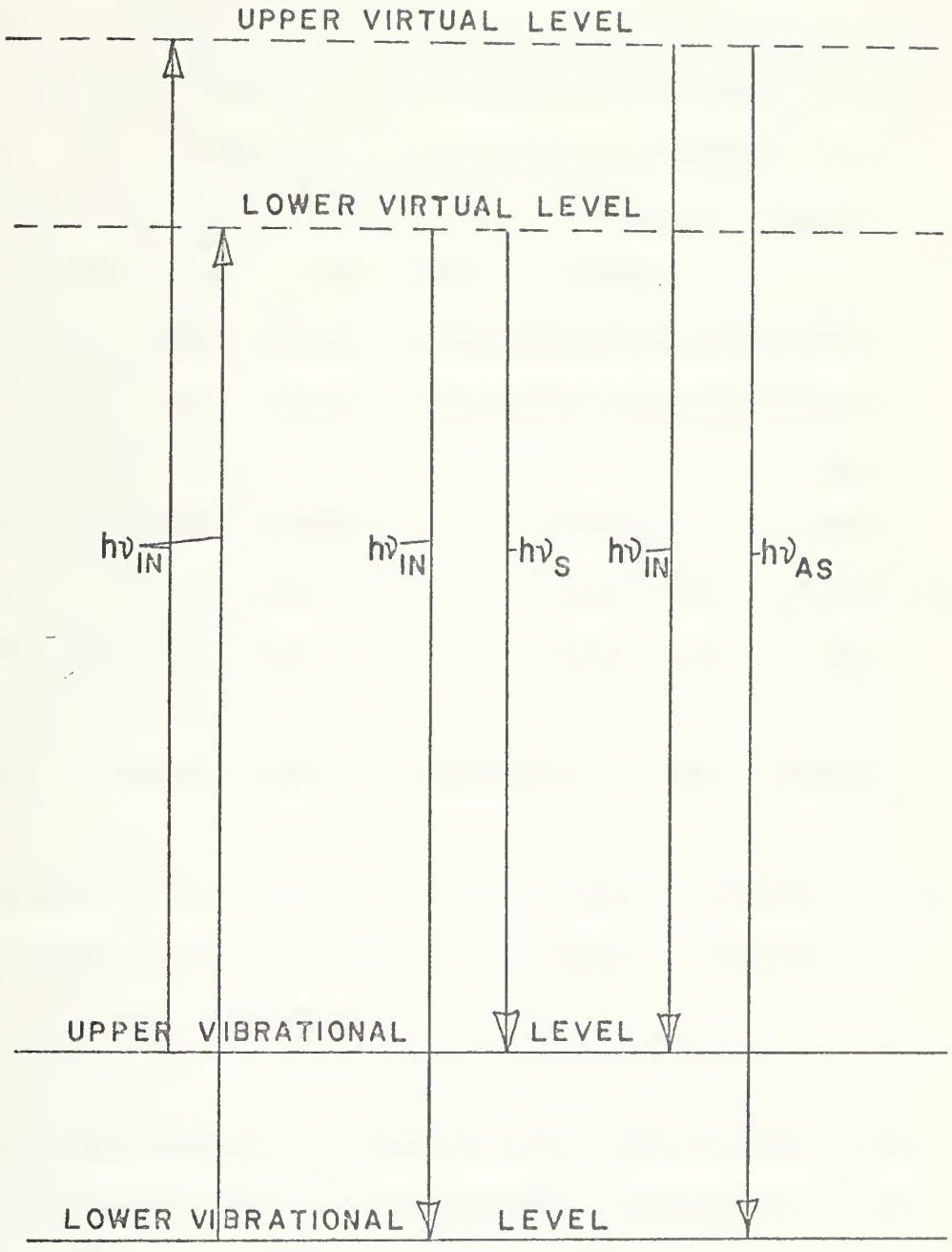

RAMAN SCATTERING

FIGURE 17

states. If there are no such levels, then the photon-molecule interaction cannot take place and it is Raman forbidden. It may be recalled that infrared spectroscopy is also dependent upon the vibrational characteristics of molecules. The infrared case deals with absorption of one photon whose energy is converted to vibrational energy, while the Raman case is a two photon process. Because of molecular or crystal symmetry considerations for highly symmetric molecules, infrared and Raman interactions are usually complementary – that is, Raman active modes are frequently infrared forbidden and vice-versa. The selection rules for the determination of active modes are derived from group theory and will not be discussed here. The thrust of the derivation, however, brings into focus the origin of the Raman effect. A material is Raman active if there is a change in the polarizability of the molecule (cf a change in the molecular electric dipole moment in the infrared active modes). Symmetric vibrational modes tend to be IR forbidden and Raman active.

The Raman effect was then, a way of observing transitions and modes of symmetric molecules that were not visible in normal infrared spectroscopy. Scientific instrument companies produced Raman spectrophotometers and these devices became standard laboratory instruments. They were quite useful for observing organic molecule's covalent bonds (cf IR observation of polar bonds) but were handicapped

somewhat because the frequency shifted light emerging from the sample was often weak and difficult to separate from the natural fluorescence that appeared in some materials. Since the Stokes lines were much more intense, they were of primary interest. The anti-Stokes lines were often treated as a scientific curiosity (or filtered out), even though they were not masked by fluorescence.

The advent of the laser touched off a new round of interest in the Raman effect. It was then possible to inject a very intense monochromatic light wave into the sample and detect modes that were previously too weak to observe. The high intensities also permitted the first observations of higher order lines which were produced by the non-linear portions of the material's polarizability. Many articles appeared reporting on the versatility of the intense, even stimulated, output for spectroscopy [84-93] and for monitoring trace elements, pollutants, flow mixing and combustion [94-97]. Since the laser beams are non-destructive, the monitoring does not affect the processes being observed. The scope of Raman Spectroscopy has increased so dramatically that a new journal, The Journal of Raman Spectroscopy, began publication in 1973.

2. Nonlinear Optics

When an electromagnetic wave interacts with an atom or molecule with bound charges, the applied electric field can induce several forms of time varying charge

separations, one of which is electronic, forming an electric dipole. This charge separation is called the electronic polarization, P. There is a proportionality between the field E and the polarization:

$$\bar{P} = \varepsilon_o \bar{\bar{\chi}}_e \bar{E} \tag{6}$$

where χ_e is the electric susceptibility. Since P and E are both vectors, χ_e is a tensor. For linear isotropic materials, the polarization follows the field direction, making χ_e a scalar. For other materials, whose geometries affect the forces involved, the polarization will not be in phase with E and may be in some direction different than E. This describes an anisotropic material. Here, χ_e must be a tensor with complex parts, if the phase is affected. Hence, we can write:

$$\chi_e = \chi_e' - i\chi e'' \tag{7}$$

Consideration of higher order terms gives

$$\bar{P}_i = \varepsilon_o \sum_j \chi_{ij}^{(1)} E_j + \varepsilon_o \sum_{jk} \chi_{ijk}^{(2)} E_j E_k + \varepsilon_o \sum_{jk\ell} \chi_{ijk\ell}^{(3)} E_j E_k E_\ell \tag{8}$$

Eq. (8) is often written in a shorthand notation:

$$\bar{P} = \varepsilon_o \left[\chi_e^{(1)} \cdot E + \chi_e^{(2)} : EE + \chi_e^{(3)} : EEE\right] \tag{9}$$

where the χ_e superscripts denote respectively, the first, second and third order susceptibilities.

In addition to the phase and directional characteristics of the susceptibility, it must also account for the vibrational and electronic resonance features that exist in bound charge systems. These resonances produce anharmonic effects at or near resonance which directly affect the susceptibility. The analysis of this nonlinear factor can be found classically using a driven, damped harmonic oscillator, or quantum mechanically. The full derivation is presented elsewhere [82, 98-100]. It is found that the total electric susceptibility can be broken up into the form of Eq. (7), such as:

$$\chi_e = \chi_e' + i\chi_e'' + \chi_{NR} \tag{10}$$

and, looking only at the third order portion,

$$\chi_e^{(3)} = \chi_e^{(3)'} + i\chi_e^{(3)''} + \chi_{NR}^{(3)} \tag{11}$$

where $\chi_{NR}^{(3)}$ is the nonresonant real portion of the susceptibility, and can be called the background susceptibility. $(\chi_e^{(3)'} + i\chi_e^{(3)''})$ is the resonant portion of the susceptibility and, according to Levenson [101]:

$$\chi_e^{(3)} = \chi^3_{NR} + \frac{N|\alpha|^2}{12h} \frac{1}{\omega_v - (\omega_1 - \omega_2) + i\Gamma} \tag{12}$$

where

α = Raman Matrix Element

ω_v = Resonant frequency of Raman active vibration

Γ = Lorentz half width at half maximum

$\omega_{1,2}$ = Frequencies of incoming laser beams

Eq. (12) is notable because as $(\omega_1 - \omega_2) \rightarrow \omega_v$, the susceptibility rises to a maximum. In some materials, where

$$\chi_{NR}^{(3)} << \frac{N|\alpha|^2}{12h\Gamma}$$

the resonant peak is quite pronounced.

The importance of the electric susceptibility becomes apparent when one considers the result of Bloembergen's [98] calculation regarding the intensity of the beam produced by mixing three photons via the nonlinear medium:

$$I_3 = \left(\frac{4\pi^2\omega_3}{c^2}\right)^2 |\chi_e|^2 I_1^2 I_2 \ell_{coh}^2 \qquad (13)$$

ℓ_{coh} is the coherence length and is defined as the distance in the sample that it takes for the wavefronts to become out of phase by π radians:

$$\ell_{coh} = \frac{\pi}{2k_1 - k_2 - k_3} \qquad (14)$$

All told, other factors being constant, the intensity of the wave at ω_3 will remain about constant (due to non-resonant real portion and small amount of the resonant part) until a Raman vibrational frequency is approached. As this frequency is attained, the intensity suddenly increases drastically to a peak at the Raman frequency, then falls off. Furthermore, by making the line width, Γ, very narrow, the effect is enhanced.

For some time during the late 1960s and early 1970s, many scientists were using this Raman resonance, as well as other resonances, to study the nonlinear processes [82,100-114]. Several, in fact, were using the $2\omega_1 - \omega_2 = \omega_3$ system which is the basis of CARS.

3. CARS

The resonances of the nonlinear susceptibility in Raman active materials offers a way of observing a measurable, strong signal-to-noise beam when three (or two) beams are adjusted so as to match the Raman vibrational frequency. In 1972, Wynne [115,116] proposed the feasibility of spectroscopy using anti-Stokes beams, as did Regnier [97] in 1973. Wynne used his procedure to study χ_e in $LiNbO_3$, and Regnier used his scattered anti-Stokes radiation (of H_2) to measure absorption of this frequency by unknown amounts of H_2 in N_2.

In 1974, Begley et. al. [117,118] demonstrated the practicality of using the resonance effect for the determination of the Raman structure of compounds. They reported an orders of magnitude increase in the conversion efficiency and a collimated output that could be easily separated from the fluorescence and the input beams. Although the method is an indirect one, it is an efficient method of avoiding the lower frequency problems while reproducing the effect.

Three photons are mixed by the Raman material to produce a fourth quantum at the anti-Stokes frequency. The process, albeit simplistically, is shown in Figure 18. Two photons at the pump frequency, ω_p, are provided by one (perhaps a dye) laser. A photon at the Stokes frequency, ω_s, is provided by a tunable dye laser. In reality, it is a concurrent mixing of four waves, through $\chi_e^{(3)}$, in any one of several different steps. Yablonovitch [111] claims that two two-wave mixing is as important as three one-wave mixing. The overall equation is:

$$2\omega_p - \omega_s = \omega_{as} \tag{15}$$

The intensity of ω_{as} in Eq. (13) is I_3, while I_1 corresponds to ω_p and I_2 to ω_s. Hence, as the Raman frequency is achieved, the maximum intensity of ω_{as} increases. Then, the difference between this and ω_p, or the difference between ω_p and ω_s, at that point, equals the Raman frequency.

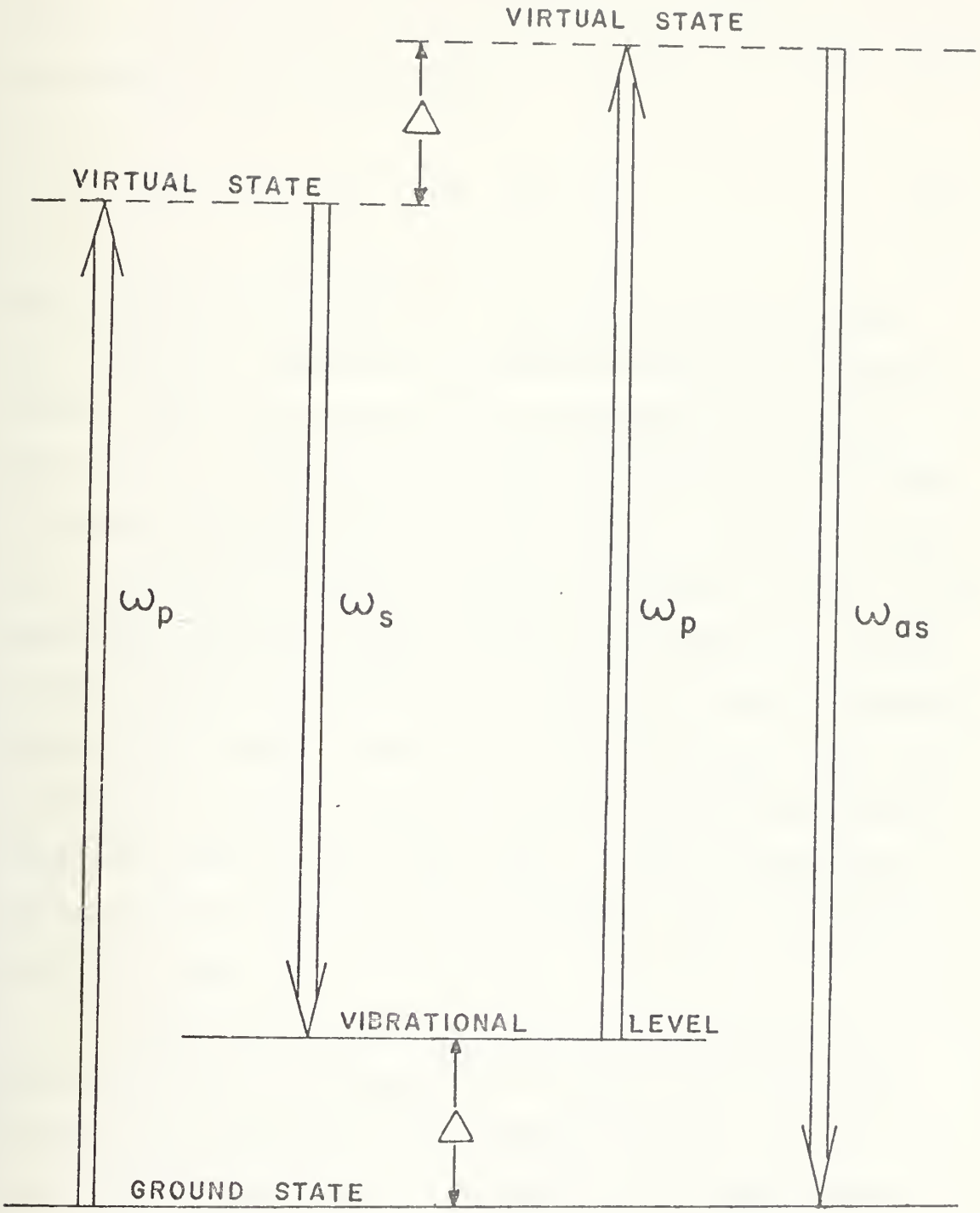

CARS ENERGY LEVEL DIAGRAM

FIGURE 18

In addition to the requirement for adhering to energy conservation as in Eq. (15), there is a phase matching requirement that must be met:

$$\Delta k = 2k_1 - k_2 - k_3, \quad \Delta k \to 0 \tag{16}$$

This is shown in Figure 19. The necessity for meeting Eq. (14) also determines the angles between the incoming beams. The output beam angle is naturally adjusted so that $\Delta k = 0$. Since the coherence length is short (~1 mm) in liquids, the angle between the beams is not as critical as it would be for gases with long coherence lengths. There are upper and lower limits for the applicability of CARS. As the frequency increases, the coherence length decreases, reducing the output intensity. The lower $\omega_{as} = 2\omega_p - \omega_s$ is limited by how accurately the anti-Stokes beam can be separated from the two input beams as their frequencies approach each other and the anti-Stokes angle approaches the other two.

Since the intensity of the anti-Stokes beam is dependent upon the intensities of both of the incoming beams, it is necessary, with current designs, to focus these input beams down to the point in the sample where the two beams cross. This provides the maximum intensity for the power provided. The size of the focal spot is approximately diffraction limited. Assuming a Gaussian

$$|\vec{K}| = \frac{\omega n}{c}$$

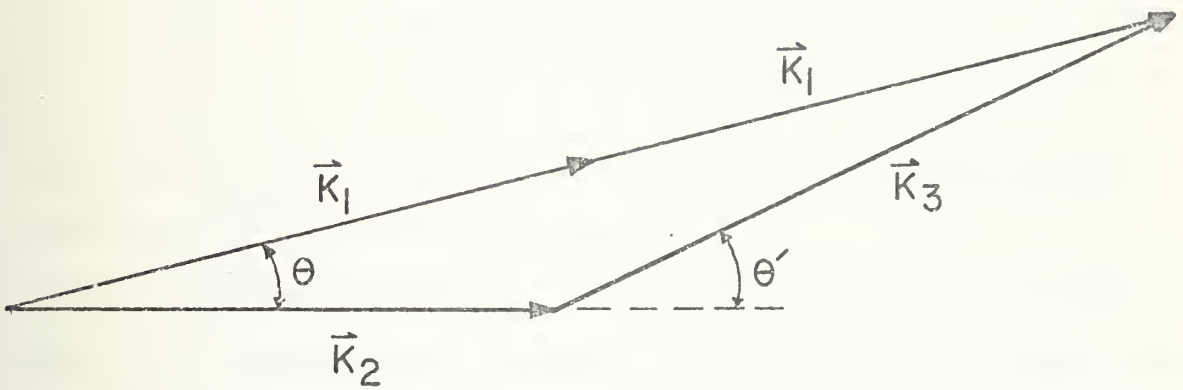

$$2\omega_1 - \omega_2 = \omega_3$$

$$2\vec{K}_1 = \vec{K}_2 + \vec{K}_3$$

PHASE MATCHING REQUIREMENT

FIGURE 19

beam:

$$w^2(z) = w_o^2[1 + (\frac{\lambda z}{\pi w_o^2})^2] \qquad (17)$$

where

$w(z)$ = Beam size at distance z

w_o = Minimum waist size of the focused beam

z = Distance from the minimum waist

and using typical values for a dye laser, the minimum spot size in the sample is ~30 micron.

For the purposes of estimating powers required for CARS, let the coherence length in Eq. (13) be two times the length at which the beam area is twice the area at the minimum waist. This is satisfied if, in Eq. (17), for

$$z = \frac{\pi w_o^2}{\lambda} , \qquad (18)$$

hence,

$$\ell_{coh} = \frac{2\pi w_o^2}{\lambda} . \qquad (19)$$

To determine the powers required,

$$I_1^2 = \frac{P_1^2}{(\pi w_o^2)^2} \tag{20}$$

Equations (19) and (20) are inserted into Eq. (13), giving

$$\frac{P_3}{P_2} = (\frac{2}{\lambda})^2 \ (\frac{4\pi^2 w_3}{c^2})^2 \ \left|\chi_e\right|^2 \ P_1^2 \tag{21}$$

As procedures, powers and concepts are improved, there is sure to be an increase in the observed conversion efficiency and more work in this area of Raman spectroscopy can certainly be expected. Recently, two reports [119, 120] appeared which may signal a new round of Raman spectroscopic investigations.

B. COHERENT ANTI-STOKES RAMAN SPECTROSCOPY: EXPERIMENTAL

The CARS equipment was set up as shown in Figure 20. Because of laboratory space limitations, this layout is slightly different than those commonly seen in the literature. Differences will be pointed out as they are encountered in the description.

The nitrogen laser must be as level as possible so that the sections following it are also all coplanar. The beam was 19 mm wide as it emerged from the laser. By the time the beam reached the beam splitting mirror, it had diverged to 30 mm. It was split so that two-thirds of the energy continued along and one-third was reflected. Other reported arrangements usually use co-linear or parallel CARS lasers.

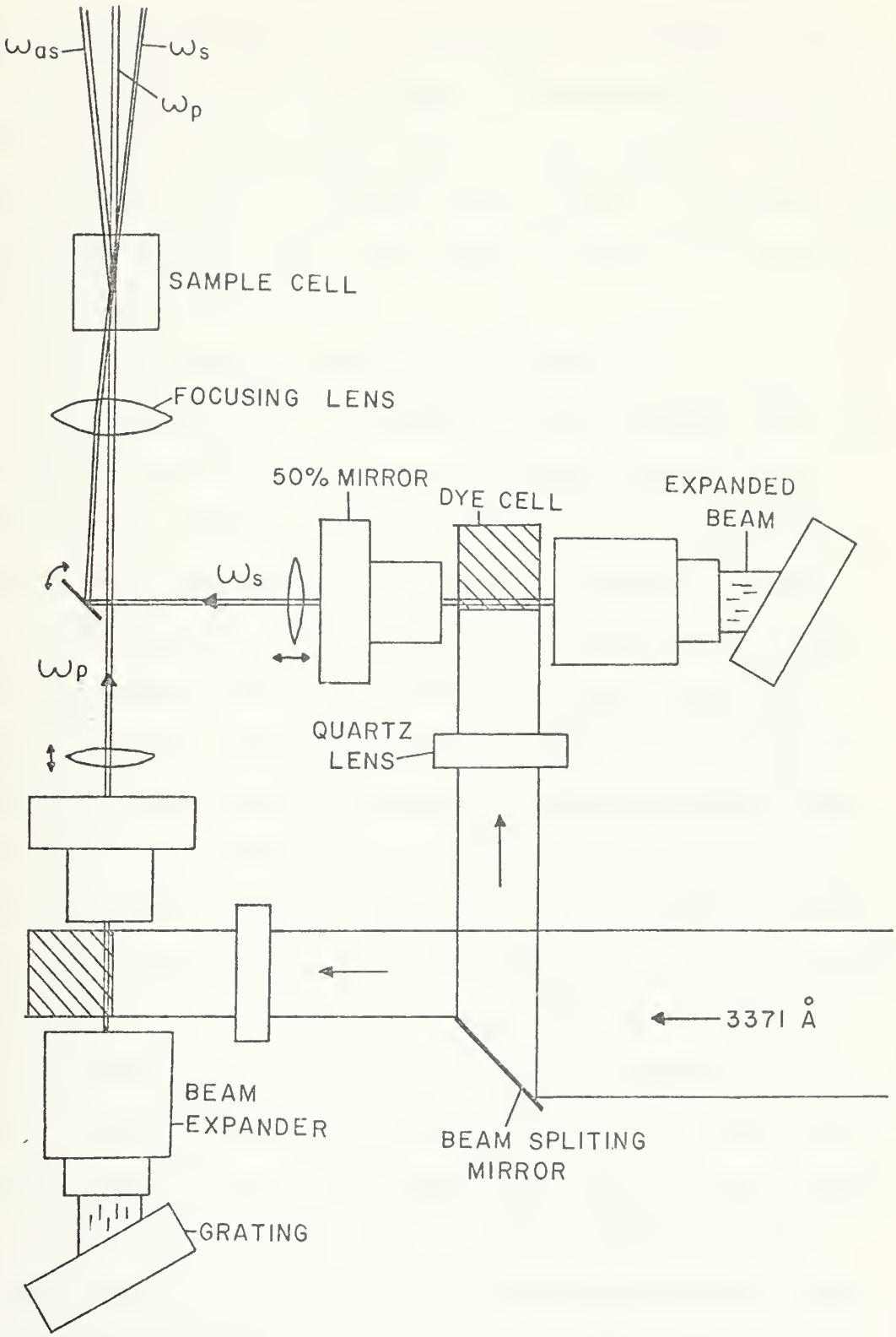

CARS APPARATUS

FIGURE 20

The 20 mm wide portion that continued on is used to pump the higher power CARS pump laser. This beam was focused into a cylindrical dye cell, as in Figure 16(A). It had been canted to prevent multiple reflections. This dye laser was aligned and its output was noted so that a second beam can later use it as a guide.

The beam splitting mirror was adjusted so that the 10 mm wide reflected beam was normal to its original direction. The distance from the uv mirror, through each dye laser system, to the sample cell was made as equal as possible. This was done to coincide, as closely as possible, the spatial pulse trains of the dye lasers' outputs when they reach the sample cell. The smaller dye cell shown in Figure 16(C) was used in the tunable laser. A larger cell would be too wide and the ultraviolet beam would not completely fill it. The tunable laser was then aligned and its output was noted. This tunable beam should cross the pump beam at the same height, or very close to it. If the height differential is too great, it will be difficult to cross the two beams later. Should the height difference be too great, it will be necessary to tilt the uv splitting mirror to adjust the height of the absorption region in the tunable laser. This will either raise or lower the beam coming from this laser. The laser must then be realigned. This is continued until the two beams cross at the same height.

A mirror was then added in the path of the tunable Stokes beam. This mirror was constructed from an aluminum coated microscope slide that had a reflectivity of 100%. It should be coated right up to the edge of the glass. The mirror slide was attached to the gimballed part of a laser mirror mount. The orthogonal adjustment feature will be critical later. The mirror was placed so that it barely missed the pump beam and yet caught the Stokes beam very close to the edge of the mirror. This mirror must be adjusted so that the two beams are as close to each other as is physically possible. The tolerance, in fact, is the factor controlling the angle of the two beams when they enter the sample. Because of this preciseness required, lenses were placed at the output of both lasers. They have focal lengths that just compensate for the beam divergence. The larger the beam, the more difficult it is to place them closely together. The reported CARS arrangements use dual gimballed mirrors so that both beams can be adjusted.

A rather short focal length lens (25 mm) was placed along the path of the pump beam and the mirror was adjusted so as to place the Stokes beam adjacent to the pump beam. This adjustment was not critical at that point. Since the position of the pump beam was fixed, it was used as the determinant for establishing the focal/crossing point. The Stokes beam was then blocked off so that only the pump beam passed through the lens. The location of its focal

point was noted visually and a card was placed at this location. The card had a 100 micron hole in it. This hole will be used to determine the correct crossing point. Once the pump focal point had been determined, the pump beam was temporarily covered and the focused Stokes beam was observed. The focal point of this beam may or may not be at the same point as the pump beam. If it is not, the lens at the Stokes output can be adjusted longitudinally to bring the Stokes beam focal point to the same location as that of the pump beam. The focal points of both beams should be at the same distance from the converging lens.

The Stokes beam was again covered and the pump beam was passed through the system. The card was placed in the beam path and was adjusted so that the maximum amount of pump radiation was passed through it. The location of the focal point can also be checked using this card. It can be moved longitudinally along the beam while observing the light that is passed through the hole. If the hole is placed directly in the middle of the beam, the maximum amount of radiation, accompanied by some diffraction patterns, can be seen on a sheet placed behind the card. The card, and hence the hole, was the point where the beams will be crossed.

The pump beam was covered and the Stokes beam was allowed to pass through. The micrometers on the mirror were carefully adjusted so that the maximum amount of Stokes light passed through the hole. At this point, it can be

determined if this is indeed the focal point of the Stokes beam, in a manner similar to that described for the pump beam. The lens on the Stokes beam should be adjusted so that the beam is focused exactly at the hole.

Both beams were then allowed to pass through the hole. Both should be fairly intense with the maximum amount of both beams passing through the hole. The mixing region had been established. The incident angle of the crossing beams can be checked by observing the separation of the beams at some distance from the crossing point. With the 25 mm lens, it was generally not possible to achieve angles less than 2.0 degrees. In order to get smaller angles, it was necessary to cut off part of the beams with the mirror. It should be mentioned that, since the focusing lens increases the crossing angle, the distance between the beams at the mirror cannot be used to determine this angle.

It would now be theoretically possible to observe the CARS effect if the card/hole is replaced by a sample cell and the tunable laser is adjusted to the proper frequency.

Since it has a very high nonlinear effect, benzene was chosen as the initial sample material. Benzene has a very strong Raman line at 992 cm^{-1}, and this line is often used as a standard. Since the Raman frequency was known, it was simply a matter of choosing dyes that would produce two laser beams that were 992 cm^{-1} apart and that would exhibit a large gain. The various combinations of wavelengths

and dyes used in this connection are shown in Table III. When work had reached this early stage, the Coumarin dyes had not been observed and so the Rhodamine 6G/Rhodamine B and Rhodamine 6G/Fluorescein combinations were attempted. Since Rhodamine B lases at longer wavelengths, it was used in the tuning laser to produce the Stokes frequency light. The Rhodamine 6G is a strong lasant and was therefore used for the pump radiation. The Fluorescein was not a strong lasant and was quickly abandoned.

Figure 15 can be used to determine the combinations of dyes and desired wavelengths. It was decided to choose wavelengths that were close to the peak powers of each dye, keeping both as high as possible. It was found that this could be done by marking off, on a card, 992 cm^{-1} to scale from the bottom of the graph and then sliding this along the two dyes contemplated until a balance of power could be attained.

In order to ascertain the exact wavelengths that the CARS apparatus was generating, a long focal length lens was inserted behind the sample cell. The emerging radiation was then focused and directed into the Jarrell-Ash Spectrometer. The procedure for approximating the Raman frequency difference was as follows: The pump laser was tuned to its proper wavelength using the value that was determined by the optimization process described above. The Stokes beam was then tuned to its correct frequency. It was verified

PUMP		STOKES	
DYE	(Å)	DYE	(Å)
Rhodamine 6G	5840	Rhodamine B	6200
"	5860	"	6222
"	5880	"	6244
"	5900	"	6267
Fluorescein	5578	Rhodamine 6G	5905
ANC-NMe	5575	Rhodamine 6G	5901
"	5626	"	5958
"	5654	"	5990
"	5690	"	6030
"	5693	"	6034

CARS WAVELENGTHS ATTEMPTED

TABLE III

that the difference between these two beams was 992 cm^{-1} ± 6 cm^{-1} (2Å). When benzene, in a cylindrical quartz cell, was placed at the crossing point, no anti-Stokes beam was apparent. Dr. A. Harvey [117,118] suggested the following procedure: A hole was punched in a piece of cardboard. This hole was placed at the approximate position where the anti-Stokes beam should appear. At the same time, the emerging beams struck the cardboard and were thus "filtered out." The active region of the benzene was then viewed straight on through the hole. A small amount of radiation in the green region could be seen, but there was no semblance of a collimated beam. Still looking into the benzene cell, the Stokes laser was tuned slowly through 24 cm^{-1} on each side of the calculated correct frequency. The green color was observed to increase through the center frequency and then fade out, but no anti-Stokes laser beam was seen.

It was possible that the two beams were not exactly crossed into each other. The established mirror setting was noted. Since there were now two variables (tuned wavelength and mirror setting), the mirror was moved in very small increments in a slowly expanding square spiral. At each increment, the Stokes beam was tuned through a reasonable range. The maximum radiation was seen at 998 cm^{-1} and at a mirror setting only slightly off that determined by the alignment procedure.

Since the CARS device had never been actually seen in operation, it was not known how the necessary powers appeared visually. The powers of the two beams appeared to be quite low, so they were measured. Although the power meter would not come to rest because of electromagnetic interference from the nitrogen laser, it did indicate that about 2-3 kW of power was being obtained from the pump laser and a much smaller and indeterminant amount of power from the Stokes laser. These were much less than those reported in the literature. It was also known that the bandwidth of the laser outputs were on the order of 12 cm^{-1}. Hence, a great deal of the available power was located in the band wings. It was decided to order larger beam expanders in order to narrow the bandwidth. The power problem was more basic and much more difficult to remedy.

Two alternatives were immediately available to increase the output powers. The most obvious solution was to increase the power of the nitrogen laser. This was discussed earlier and proved to be more basic and difficult than was at first thought. The choice of wavelengths and dyes was another possible solution. To this end, the wavelengths of the two dyes were changed, maintaining the proper frequency difference, in an attempt to squeeze more total output power out of the system. The improvement was negligible, mainly because of the relatively low gain of the Rhodamine B.

At that point, the Coumarins obtained from NWC and NELC were pumped and measured. The ANC-NMe showed

remarkably high gain in the yellow region of the spectrum. It was decided to reverse the role of the Rhodamine 6G. The ANC-NMe was placed in the pump laser and the Rhodamine 6G was placed in the Stokes laser. The outputs were shifted to shorter wavelengths from the earlier combination and the powers appeared much stronger, especially that of the Stokes beam. The pump beam power was ~5 kW while the Stokes was ~2 kW. The fluorescence appearing in the benzene cell was stronger, but the increase was not dramatic and there was still no indication of a collimated anti-Stokes beam.

The other solution was to decrease the laser bandwidth. To this end, new lenses were inserted in the beam expanders. These lenses enabled more of the grating areas to be utilized, thereby reducing the bandwidth of the tuned output. The optical bandwidth was then approximately 2Å. It was possible that the true bandwidth value may be lower, as the grating in the spectrometer was not fully utilized. Although 2 Å was still rather wide for spectroscopic purposes, the amount of radiated energy per unit wavelength was doubled. Further decreases in the spectral output could be provided by the use of etalons (which were available). When these narrowed beams were focused into the sample, an increase in the amount of green anti-Stokes radiation was noted, but no collimated beam was apparent.

In order to evaluate how well the apparatus should theoretically perform, Eqs. (13) and (21) were analyzed

using parameters typical of the lasers being used. During the alignment process, it was estimated that the beam waist was far from the diffraction limited case. It was visually determined that the beam was approximately 100 μ wide at its focal point. This larger beam has two effects in Eq. (13). The effective coherence length increases and the intensity decreases.

In order to determine the effects of a focal point that is not diffraction limited, Figure 21 was used to visualize the parameters. w_o is the waist size of the diffraction limited beam, while w is the radius of this beam at any other point, z. w' is the radius of any other beam. The difference at any point is a:

$$w' = w + a \ , \tag{22}$$

and

$$w'(z)^2 = w(z)^2 + 2w(z)\ a + a^2$$

$$= w_o^2 \left(1 + \frac{\lambda z}{\pi w_o^2}\right) + 2w_o a \sqrt{1 + \frac{\lambda z}{\pi w_o^2}} + a^2 \tag{23}$$

It was desired to determine the point where the area of the non-limited beam was equal to twice the area of the waist size of the nonlimited beam:

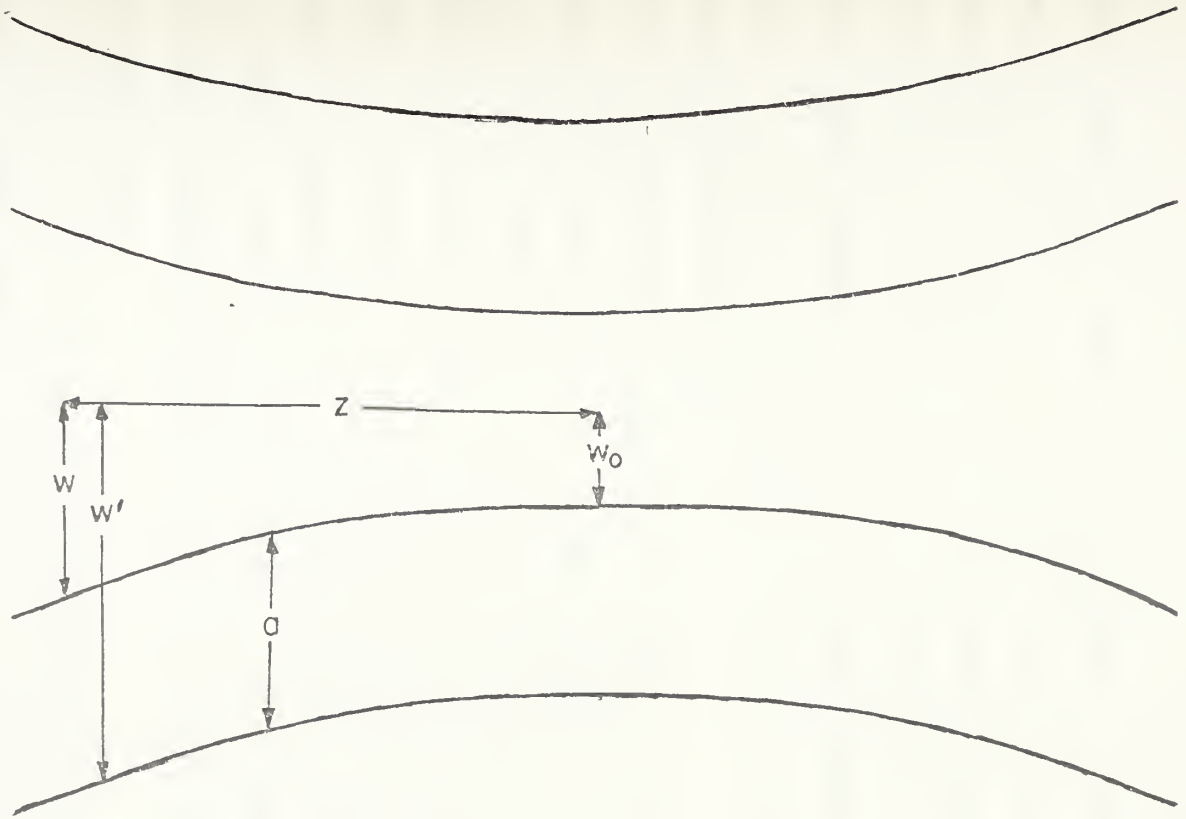

FIGURE 21

BEAM WAIST

$$\frac{w'(z)^2}{w'(0)^2} = 2 = \frac{w_o^2\left(1 + \frac{\lambda z}{\pi w_o^2}\right) + 2w_o a\sqrt{1 + \frac{\lambda z}{\pi w_o^2}} + a^2}{w_o^2 + 2w_o a + a^2} \qquad (24)$$

Using typical values of 10 μ for the diffraction limited waist and 100 μ for the waist of the laser beam in use, it was calculated that in this experiment, the output intensity would be only 1.82×10^{-2} times that of the limited case. Assuming that the Stokes beam had a power of 4 kW, the anti-Stokes output would be only about 4 W. One of these pulses would contain approximately 10^{10} photons. This is considerably more than is required for detection by the human eye.

It was also observed that the quality of the dye laser beams was far from perfect. There appeared to be a complicated mode structure. The lower beam qualities directly affected the phase matched interactions occuring in the benzene. Instead of a smooth, even mixing, a time-varying series of interactions were believed to be taking place. It is obvious that this would result in the production of a diffuse pattern of radiation rather than a well defined, collimated beam.

It is believed, then, that the radiation that was observed coming from the interaction area was indeed the result of the anti-Stokes process. Although the exact wavelength of this light could not be determined, it was visually verified that the color was very close to the

wavelength that was calculated. The fact that the intensity of this radiation increased and then decreased as the dye beam was swept through the Raman frequency and as the adjustment mirror was rotated reinforces this belief.

At this time, it was realized that the effects of refraction, due to the benzene, had not been taken into account. Benzene has an index of refraction of 1.502. This affects the manner in which the incoming beams are crossed and focused. Previously, the alignment of the crossed beams had been determined using a hole in air. The sample cell was then installed. It had been assumed that the focal points and crossing point remained constant during the addition of the cell. In fact, because of the refraction, the crossing point was shifted to a point further away from the lens. If the plane of the two beams was not normal to the sample cell, the beams would be uncrossed as they travelled through the sample cell. The solution was obvious. A small hole was placed in a strip of aluminum foil. This foil could then be lowered into the sample and the beams could be focused and crossed in the Raman active material's own environment. This was never done as multiple problems were being encountered with the nitrogen laser and adequate dye laser output power could not be achieved.

It was also at this point that the degradation of Coumarin dyes was observed. The output of the strong dye

laser beam had been gradually decreasing as the laser was repetitively fired. Finally, the ANC-NMe would no longer lase. The solution had turned from a yellow color to an orange color. As the small amount of solution in use represented the total amount of the dye that was available, other alternatives were investigated. A pump beam in the yellow region was desired. No currently used dyes have their maximum outputs around 5900 Å, so it was recommended that small amounts of Disodium Fluorescein be added to Rhodamine 6G in order to enhance the yellow output.

V. SUMMARY

The results reported in this paper demonstrate that Coherent Anti-Stokes Raman Spectroscopy can be observed on a small scale under less than optimum conditions. This fact, in itself, is important in that it shows that the effect is of sufficient magnitude to be observable in a number of situations. Even with extremely low conversion efficiencies, the anti-Stokes output is visible. With a series of modifications designed to increase this efficiency, the output could become fairly strong for observations of low concentrations and weak lines.

The design, construction and improvement of the several types of lasers used in the apparatus proved to be the most frustrating, yet educational portion of the research. In order to find a nitrogen laser with the highest power, it was necessary to analyze several of the many designs that have been reported in the literature. In most cases, the output powers that were observed did not approach the reported values. Nevertheless, one of the lasers that was constructed produced nanosecond pulses with peak powers that ranged up to 160 kW.

The outputs of the dye lasers amply demonstrate that fully tunable coherent sources can be developed by individuals requiring such a device. The high gain and short pulses result in reasonably high peak powers that can be used for a variety of spectroscopic studies.

The appearance of the anti-Stokes radiation caused by the interaction of the dye laser beams in the Raman active material did not resemble that reported in the literature. This was undoubtedly caused by the beam qualities present in the apparatus used. However, it would be possible to obtain the coherent output with a modest number of improvements to the system.

VI. SUGGESTIONS FOR FUTURE EFFORTS

When developing new concepts and equipment, a great deal of time and expertise must be devoted to achieve the ultimate goal. Such was the case in the proceedings reported in this paper. The theory and application of nitrogen lasers, even at the most advanced levels of industrial technology, is, at best, incomplete and far from being perfect. It was therefore necessary to invest a considerable amount of effort to construct, from scratch, a viable and efficient dye laser pump. Without this concrete base, the remainder of the experiment is moot.

Each of the three nitrogen laser systems investigated had its own advantages and drawbacks. The Nagata laser was simple to construct and was quite reliable, once the stray inductances had been removed. It suffered from severe arcing problems and a low output power. With some modifications, it is believed, however, that this design could become the most effective. The 38 cm active region should be extended to 80-90 cm to take advantage of the optimal dB vs length values reported in the literature. If thicker electrodes were incorporated in the design, the edges could be rounded using a larger radius of curvature and the arcing may be reduced. A larger flow rate (using larger capacity pumps) would compensate for the additional

volume of gas in the cell. The large number of individual storage capacitors would provide for replacement of discrete failures. Since the "traveling wave effect" has been ruled out in this experiment, it is felt that a continuous capacitor plate is unnecessary.

The Schenck laser is advantageous in that it can be accurately fired at any specific repetition rate. With some design changes, the transmission line deficiencies could be remedied. The remainder of the shortcomings are similar to those of the Nagata laser and similar solutions could be attempted.

The Godard laser, which received the greatest share of time and effort, proved to be, simultaneously, the most valuable for basic nitrogen laser research and the least valuable when a consistant, reliable laser energy source was required. Its design enabled the researcher to perform on-the-spot modifications to improve performance. Its modular design allowed a systematic evaluation of each of its components to be conducted. As a result of this, the parabolic shape was discounted, the deficiencies of the dielectric material were discovered and the thick electrode was verified as the way to defeat the arcing problem. This laser, however, would not operate for any great lengths of time and this fact contributed significantly to the fact that more effort was not expended in the CARS research. At

least 24 hours was required to repair board damages and, with the added offset edges and rounded corners, two to three days were needed to etch each board. This time represented a considerable amount of dead time that could not be used to improve the final result.

The dye laser design was fairly straightforward and will require only minimum modifications in the future. The aluminum and silver coated microscope slides degrade with age and have to be replaced at regular intervals. These mirrors cannot be accurately reproduced and have not been specifically designed to reject wideband super-radiance while passing the desired tuned wavelengths. This factor is not critical but commercially produced dye laser mirrors could produce better beam mode structure and wavelength selectivity. If necessary, etalons should be added to the laser cavity to further reduce the laser bandwidths. Again, this factor is not necessary if sufficient powers are available.

Assuming that operational laser powers can be obtained, the foil-in-sample alignment method discussed earlier should be followed. This could provide the means necessary to observe the effect described herein. It may also be necessary to stabilize the mount alignment of the grating orientation. Any mount deficiencies result in constant adjustments being required during tuning. This would be necessary for commercial devices where operator controls must be kept to a minimum.

When adequate Stokes and dye laser pump powers are obtained, there are many effects that should be investigated involving the crossed laser beams. Beam polarization may prove to be an important factor. Since the radiation coming off the diffraction grating is approximately polarized in the vertical direction, both beams are vertically polarized when they cross in the sample. Polarizing crystals, between the dye cell and the output mirror should pass the tuned wavelength, while eliminating at least half of the superradiant output. Downline quarter wave plates and polarizers will enable further studies of the effect of the wave orientation on the susceptibility tensor.

During the course of the CARS experiment, a Neodymium filter was used to eliminate the strong yellow line so that the anti-Stokes line could be observed. When this filter was tested on a spectrometer, it was discovered that a relatively strong secondary absorption line existed in the region where the anti-Stokes line should have occurred. This filter could be used to an advantage, however. If the yellow pump beam could be set to exactly fit the filter, the anti-Stokes line will fall outside of the filter's secondary absorption line. This would facilitate the observation of the CARS effect, in benzene at least. Other filter methods will have to be developed if this system it to be used on Raman active materials in general.

It appears that, with modifications that have been determined during the course of this research, a moderately inexpensive, easy to construct CARS device can be developed by any reasonably equipped laboratory. This apparatus can be used to study a variety of effects, such as dye laser chemistry, material nonlinearities, including higher orders using higher powers, crystal symmetries and the CARS described in this report.

LIST OF REFERENCES

1. Sorokin, P. P., and Lankard, J. R., "Stimulated Emission Observed from an Organic Dye, Chloro-Aluminum Phtalocyanine," IBM Journal of Research and Development, Vol. 10, p. 162-163, March 1966.

2. Schäfer, F. D., Werner, S., and Volze, J., "Organic Dye Solution Laser," Applied Physics Letters, Vol. 9, p. 306-309, 15 October 1966.

3. Spaeth, M. L., and Bortfeld, D. P., "Stimulated Emission from Polymethine Dyes," Applied Physics Letters, Vol. 9, p. 179-181, 1 September 1966.

4. Schäfer, F. P., Schmidt, W., and Marth, K., "New Dye Lasers Covering the Visible Spectrum," Physics Letters, Vol. 24A, p. 280-281, 27 February 1967.

5. Sorokin, P. P., Lankard, J. R., Hammond, E. C. and Moruzzi, V. L., "Laser-Pumped Stimulated Emission from Organic Dyes: Experimental Studies and Analytical Comparisons," IBM Journal of Research and Development, Vol. 11, p. 130-147, March 1967.

6. McFarland, B. B., "Laser Second-Harmonic-Induced Stimulated Emission of Organic Lyes," Applied Physics Letters, Vol. 10, p. 208-209, 1 April 1967.

7. Glenn, W. H., Brienza, M. J., and DeMaria, A. J., "Mode Locking of an Organic Dye Laser," Applied Physics Letters, Vol. 12, p. 54-56, 15 January 1968.

8. Soffer, B. H., and Linn, J. W., "Continuously Tunable Picosecond-Pulse Organic-Dye Laser," Journal of Applied Physics, Vol. 39, p. 3859-3860, December 1968.

9. DeMaria, A. J., Glenn, W. H., Jr., Brienza, M. J., and Mack, M. E., "Picosecond Laser Pulses," Proceedings of the IEEE, Vol. 57, p. 2-25, January 1969.

10. Sorokin, P. P., and Lankard, J. R., "Flashlamp Excitation of Organic Dye Lasers: A Short Communication," IBM Journal of Research and Development, Vol. 11, p. 148, March 1967.

11. Schmidt, W., and Schäfer, F. P., "Self-Mode-Locking of Dye-Lasers with Saturable Absorbers," Physics Letters, Vol. 26A, p. 558-559, 22 April 1968.

12. Snavely, B. B., Peterson, O. G., and Reithel, R. F., "Blue Laser Emission from a Flashlamp-Excited Organic Dye Solution," Applied Physics Letters, Vol. 11, p. 275-276, 1 November 1967.

13. Deutsch, T. F., Bass, M., and Meyer, P., "Emission Spectrum of Rhodamine B Dye Lasers," Applied Physics Letters, Vol. 11, p. 379-381, 15 December 1967.

14. Schimitschek, E. J., Nehrich, R. B., and Trias, J. A., "Recirculating Liquid Laser," Applied Physics Letters, Vol. 9, p. 103-104, 1 August 1966.

15. Sorokin, P. P., Lankard, J. R., Moruzzi, V. L., and Hammond, E. C., "Flashlamp-Pumped Organic-Dye Lasers," Journal of Chemical Physics, Vol. 48, p. 4726-4741, 15 May 1968.

16. Drake, J. M., Tam, E. M., and Morse, R. I., "The Use of Light Converters to Increase the Power of Flashlamp-Pumped Dye Lasers," IEEE Journal of Quantum Electronics, Vol. QE-8, p. 92-94, February 1972.

17. Hänsch, T. W., Schawlow, A. L., and Toschek, P., "Simple Dye Laser Repetitively Pumped by a Xenon Ion Laser," IEEE Journal of Quantum Electronics, Vol. QE-9, p. 553-554, May 1973.

18. Bridges, W. B., "Laser Action in Single Ionized Krypton and Xenon," Proceedings of the IEEE, Vol. 52, p. 843-844, July 1964.

19. Hoffman, V., and Toscheck, P., "New Laser Emission from Ionized Xenon," IEEE Journal of Quantum Electronics, Vol. QE-6, p. 648-649, October 1970.

20. Peterson, O. G., Tuccio, S. A., and Snavely, B. B., "On Operation of an Organic Dye Solution Laser," Applied Physics Letters, Vol. 17, p. 245-247, 15 September 1970.

21. Hercher, M., and Pike, H. A., "Continuous Dye Laser Emission from 5220 to 6570 A," IEEE Journal of Quantum Electronics, Vol. QE-7, p. 473, September 1971.

22. Kogelnik, H. W. Ippen, E. P., Dienes, A., and Shank, C. V., "Astigmatically Compensated Cavities for cw Dye Lasers," IEEE Journal of Quantum Electronics, Vol. QE-8, p. 373-379, March 1972.

23. Runge, P. K., and Rosenberg, R., "Unconfined Flowing-Dye Films for cw Dye Lasers," IEEE Journal of Quantum Electronics, Vol. QE-8, p. 910-911, December 1972.

24. Dienes, A., Ippen, E. P., and Shank, C. V., "High-Efficiency Tunable cw Dye Laser," IEEE Journal of Quantum Electronics, Vol. QE-8, p. 388, March 1972.

25. Dienes, A., Ippen, E. P., and Shank, C. V., "A Mode-Locked cw Dye Laser," Applied Physics Letters, Vol. 19, p. 258-260, 15 October 1971.

26. Kuizenga, D. J., "Mode Locking of the cw Dye Laser," Applied Physics Letters, Vol. 19, p. 260-263, 15 October 1971.

27. Shah, J., "New Output Coupling Scheme for cw Dye Lasers," Applied Physics Letters, Vol. 20, P. 479-480, June 1972.

28. Ippen, E. P., Shank, C. V., and Dienes, A., "Passive Mode Locking of the cw Dye Laser," Applied Physics Letters, Vol. 21, p. 348-350, October 1972.

29. Lankard, J. R., and von Gutfeld, R. J., "Organic Lasers Excited by a Pulsed N_2 Laser," IEEE Journal of Quantum Electronics, Vol. QE-5, p. 625, December 1969.

30. Lidholt, L. R., "Dye Laser Pumped by an Ultraviolet Nitrogen Laser," IEEE Journal of Quantum Electronics, Vol. QE-6, p. 162, March 1970.

31. Myers, J. A., Johnson, C. L., Kierstead, E., Sharma, R. D., and Itzkan, I., "Dye Laser Stimulation with a Pulsed N_2 Laser Line at 3371 A," Applied Physics Letters, Vol. 16, p. 3-5, 1 January 1970.

32. Broida, H. P., and Haydon, S. C., "Ultraviolet Laser Emission of Organic Liquid Scintillators Using a Pulsed Nitrogen Laser," Applied Physics Letters, Vol. 16, p. 142-144, 1 February 1970.

33. Shank, C. V., Dienes, A., Trozzola, A. M., and Myer, J. A., "Near uv to Yellow Tunable Laser Emission From an Organic Dye," Applied Physics Letters, Vol. 16, p. 405-407, 15 May 1970.

34. Shank, C. V., Dienes, A., and Silfvast, W. T., "Single Pass Gain of Exciplex 4-mu and Rhodamine 6G Dye Laser Amplifiers," Applied Physics Letters, Vol. 17, p. 307-309, 1 October 1970.

35. Hänsch, T. W., Varsanyi, F., and Schawlow, A. L., "Image Amplification by Dye Lasers," Applied Physics Letters, Vol. 18, p. 108-110, 15 February 1971.

36. Godard, B., "A Simple High-Power Large-Efficiency N_2 Ultraviolet Laser," IEEE Journal of Quantum Electronics, Vol. QE-10, p. 147-153, February 1974.

37. Willett, C. S., and Litynski, D. M., "Power Increase of N_2 uv and ir Lasers by Addition of SF_6," Applied Physics Letters, Vol. 26, p. 118-120, 1 February 1975.

38. Heard, H. G., "Ultraviolet Gas Laser at Room Temperature," Nature, Vol. 200, p. 667, 16 November 1963.

39. Heard, H. G., "High Power Ultraviolet Gas Laser," Bulletin of the American Physical Society, Vol. 9, p. 65, 1964.

40. Leonard, D. A., "Saturation of the Molecular Nitrogen Second Positive Laser Transition," Applied Physics Letters, Vol. 7, p. 4-6, 1 July 1965.

41. Gerry, E. T., "Pulsed-Molecular-Nitrogen Laser Theory," Applied Physics Letters, Vol. 7, p. 6-8, 1 July 1965.

42. Ali, A. W., Kolb, A. C., and Anderson, A. D., "Theory of the Pulsed Molecular Nitrogen Laser," Applied Optics, Vol. 6, p. 2115-2119, December 1967.

43. Shipman, J. D., Jr., "Traveling Wave Excitation of High Power Gas Laser," Applied Physics Letters, Vol. 10, p. 3-4, 1 January 1967.

44. Geller, M., Altman, D. E., and DeTemple, T. A., "A Pulsed, Coaxial Transmission Line Gas Laser," Journal of Applied Physics, Vol. 37, p. 3639-3640, 1966.

45. Ericsson, K. G., and Lidholt, L. R., "Ultraviolet Source with Repetitive Subnanosecond Kilowatt Pulses," Applied Optics, Vol. 7, p. 211, January 1968.

46. Geller, M., Altman, D. E., and DeTemple, T. A., "Some Considerations in the Design of a High Power, Pulsed N_2 Laser," Applied Optics, Vol. 7, p. 2232-2237, November 1968.

47. Phillips, D. T., and West, J., "The Poor Man's Nitrogen Laser," American Journal of Physics, Vol. 38, p. 655-657, May 1970.

48. Small, J. G., and Ashari, R., "A Simple Pulsed Nitrogen 3371 A Laser with a Modified Blumlein Excitation Method," The Review of Scientific Instruments, Vol. 43, p. 1205-1206, August 1972.

49. Woodward, B. W., and Ehlers, V. J., "A Reliable, Repetitively Pulsed, High-Power Nitrogen Laser," The Review of Scientific Instruments, Vol. 44, p. 882-887, July 1973.

50. Stephenson, P. B., and McDowell, V. P. "A Dual Channel Nitrogen Laser Useful for Nanosecond Excited State Studies," The Review of Scientific Instruments, Vol. 45, p. 427-428, March 1974.

51. Nagata, I., and Kumura, Y., "A Compact High-Power Nitrogen Laser," Journal of Physics E: Scientific Instruments, Vol. 6, p. 1193-1195, 1973.

52. Schenck, D., and Metcalf, H., "Low Cost Nitrogen Laser Design for Dye Laser Pumping," Applied Optics, Vol. 12, p. 183-186, February 1973.

53. Levatter, J. I., and Lin, S-C., "High-Power Generation from a Parallel-Plates-Driven Pulsed Nitrogen Laser," Applied Physics Letters, Vol. 25, p. 703-705, 15 December 1974.

54. Kurnit, N. A., Tubbs, S. J., Bidhichand, K., Ryan, L. W.,Jr., and Javan, A., "Photopreionization of the 3371-A Pulsed N_2 Laser," IEEE Journal of Quantum Electronics, Vol. QE-11, p. 174-176, April 1975.

55. Suchard, S. N., Galvan, L., and Sutton, D. G., "Quasi-cw Laser Emission from the Second Positive Band of Nitrogen," Applied Physics Letters, Vol. 26, p. 521-523, 1 May 1975.

56. Schäfer, F. P. (Ed.), and others, Topics in Applied Physics: Dye Lasers, p. 1, Springer-Verlag, 1973.

57. Rautian, S. G., and Sobel'man, I. I., "Remarks on Negative Absorption," Optics and Spectroscopy, Vol. 10, p. 65-66, January 1961.

58. Stockman, D. L., Mallory, W. R., and Tittel, K. F., "Stimulated Emission in Aromatic Organic Compounds," Proceedings of the IEEE, Vol. 52, p. 318-319, March 1964.

59. Bradley, D. J., Durrant, A. J. F., Gale, G. M., Moore, M., and Smith, P. D., "Characteristics of Organic Dye Lasers as Tunable Frequency Sources for Nanosecond Absorption Spectroscopy," IEEE Journal of Quantum Electronics, Vol. QE-4, p. 707-711, November 1968.

60. Walther, H., and Hall, J. L., "Tunable Dye Laser with Narrow Spectral Output," Applied Physics Letters, Vol. 17, p. 239-242, 15 September 1970.

61. Okada, M., Shimizu, S., and Ieiri, S., "Tuning of a Dye Laser by a Birefringent Fabry-Perot Etalon," Applied Optics, Vol. 14, p. 917-922, April 1975.

62. Holtom, G., and Teschke, O., "Design of a Birefringent Filter for High Power Dye Lasers," IEEE Journal of Quantum Electronics, Vol. QE-10, p. 577-579, August 1974.

63. Soffer, G. H., and McFarland, B. B., "Continuously Tunable, Narrow-Band Organic Dye Lasers," Applied Physics Letters, Vol. 10, p. 266-267, 15 May 1967.

64. Shank, C. V., Bjorkholm, J. E., and Kogelnik, H., "Tunable Distributed-Feedback Dye Laser," Applied Physics Letters, Vol. 18, p. 395-396, 1 May 1971.

65. Strome, F. C., and Webb, J. P., "Flashtube-Pumped Dye Laser with Multiple-Prism Tuning," Applied Optics, Vol. 10, p. 1348-1353, June 1971.

66. Bradley, D. J., Caughey, W. G. I., and Vukusic, J. I., "High Efficient Interferometric Tuning of Flashlamp Pumped Dye Lasers," Optics Communications, Vol. 4, p. 150-153, October 1971.

67. Myers, S. A., "An Improved Line Narrowing Technique for a Dye Laser Excited by a Nitrogen Laser," Optics Communications, Vol. 4, p. 187-189, October 1971.

68. Bjorkholm, J. E., Damen, T. C., and Shah, J., "Improved Use of Gratings in Tunable Lasers," Optics Communications, Vol. 4, p. 283-284, December 1971.

69. Chandra, S., Takeuchi, N., and Hartman, S. R., "Prism-Dye Laser," Applied Physics Letters, Vol. 21, p. 144-146, 15 August 1972.

70. Marowsky, G., Tittel, F. K., and Schäfer, F. P., "Prism Tuner for Single Frequency Operation of a cw Dye Laser," Optics Communications, Vol. 13, p. 100-103, February 1975.

71. Marotta, A., and Arguello, C. A., "Dye Ring Laser Narrowing and Tuning Using the Optical Activity Dispersion of Crystal Quartz," Optics Communications, Vol. 13, p. 226-230, March 1975.

72. Jain, K., Wozniak, W. T., and Klein, M. V., "Diffraction Grating Use to Reject Fluorescence from a Tunable Dye Laser," Applied Optics, Vol. 14, p. 811-812, April 1975.

73. Hard, T. M., "Laser Wavelength Selection and Output Coupling by a Grating," Applied Optics, Vol. 9, p. 1825-1830, August 1970.

74. Hänsch, T. W., "Repetitively Pulsed Tunable Dye Laser for High Resolution Spectroscopy," Applied Optics, Vol. 11, p. 895-898, April 1972.

75. DeTemple, T. A., Plant, T. K., and Coleman, P. D., "Intense Superradiant Emission at 496 nm from Optically Pumped Methyl Fluoride," Applied Physics Letters, Vol. 22, p. 644-646, 15 June 1973.

76. Schimitschek, E. J., Trias, J. A., Taylor, M., and Celto, J. E., "New Improved Laser Dye for the Blue-Green Spectral Region," IEEE Journal of Quantum Electronics, Vol. QE-9, p. 781-782, July 1973.

77. Hildebrand, O., "Nitrogen Laser Excitation of Polymethine Dyes for Emission Wavelengths up to 9500 A," Optics Communications, Vol. 10, p. 310-312, April 1974.

78. Marling, J. B., Hawley, J. G., Liston, E. M., and Grant, W. D., "Lasing Characteristics of Seventeen Visible-Wavelength Dyes using a Coaxial-Flashlamp-Pumped Laser," Applied Optics, Vol. 13, p. 2317-2320, October 1974.

79. Castelli, F., "Stimulated Emission of Cresyl Violet Pumped by N_2 laser or Rhodamine 6G Dye Laser," Applied Physics Letters, Vol. 26, p. 18-19, 1 January 1975.

80. Reynolds, G. A., and Drexhage, K. H., "New Coumarin Dyes with Rigidized Structure for Flashlamp-Pumped Dye Lasers," Optics Communications, Vol. 13, p. 222-225, March 1975.

81. Webb, J. P., Webster, F. G., and Plourde, B. E., "Sixteen New IR Laser Dyes," IEEE Journal of Quantum Electronics, Vol. QE-11, p. 114-119, March 1975.

82. Maker, P. D., and Terhune, R. W., "Study of Optical Effects Due to an Induced Polarization Third Order in the Electric Field Strength," Physical Review, Vol. 137, p. A801-A818, 1 February 1965.

83. Anderson, A., The Raman Effect, p. 3, Marcel Dekker, Inc., 1971.

84. Chiao, R., and Stoicheff, B. P., "Angular Dependence of Maser Stimulated Raman Radiation in Calcite," Physical Review Letters, Vol. 12, p. 290-293, 16 March 1964.

85. Walrafen, G. E., "Raman Spectral Studies of Water Structure," The Journal of Chemical Physics, Vol. 40, p. 3249-3256, 1 June 1964.

86. Lallemand, P., Simova, P., and Bret, G., "Pressure-Induced Line Shift and Collisional Narrowing in Hydrogen Gas Determined by Stimulated Raman Emission," Physical Review Letters, Vol. 17, p. 1239-1241, 19 December 1966.

87. Walrafen, G. E., "Raman Spectral Studies of the Effects of Temperature on Water Structure," The Journal of Chemical Physics, Vol. 47, p. 114-126, 1 July 1967.

88. Skinner, J. G., and Nilson, W. G., "Absolute Raman Scattering Cross-Section Measurement of the 992 cm^{-1} Line of Benzene," Journal of the Optical Society of America, Vol. 58, p. 113-119, January 1968.

89. Tobin, M. C., "Laser Raman Spectroscopy of Crystal Powders," Journal of the Optical Society of America, Vol. 58, p. 1057-1061, August 1968.

90. Delhaye, M., "Rapid Scanning Raman Spectroscopy," Applied Optics, Vol. 7, p. 2195-2199, November 1968.

91. Melveger, A. J., Brasch, J. W., and Lippincott, E. R., "Laser Raman Spectra of Liquid and Solid Bromine and Carbon Disulfide under High Pressure," Applied Optics, Vol. 9, p. 11-15, January 1970.

92. McNice, G. T., "Raman Spectroscopy with a Tunable Dye Laser and a Narrow-Band Filter," Applied Optics, Vol. 11, p. 699-700, March 1972.

93. Lukasik, J., and Ducuing, J., "Anharmonic Coherent Raman Scattering in H_2," Physical Review Letters, Vol. 28, p. 1155-1158, 1 May 1972.

94. Kobayasi, T., and Inaba, H., "Spectroscopic Detection of SO_2 and CO_2 Molecules in Polluted Atmosphere by Laser-Raman Radar Technique," Applied Physics Letters, Vol. 17, p. 139-141, 15 August 1970.

95. Hirschfeld, T., SchildKraut, E. R., Tannenbaum, H., and Tanenbaum, D., "Remote Spectroscopic Analysis of PPM-Level Air Pollutants by Raman Spectroscopy," Applied Physics Letters, Vol. 22, p. 38-40, 1 January 1973.

96. Ahmed, S. A., "Molecular Air Pollution Monitoring by Dye Laser Measurement of Differential Absorption of Atmospheric Elastic Backscatter," Applied Optics, Vol. 12, p. 901-903, April 1973.

97. Regnier, P. R., and Taran, J. P. E., "On the Possibility of Measuring Gas Concentrations by Stimulated Anti-Stokes Scattering," Applied Physics Letters, Vol. 23, p. 240-242, 1 September 1973.

98. Bloembergen, N., Nonlinear Optics, p. 1-19, Benjamin, 1965.

99. Yariv, A., Introduction to Optical Electronics, Holt, Rinehart and Winston, 1971.

100. Armstrong, J. A., Bloembergen, N., Ducuing, J., and Pershan, P. S., "Interactions Between Light Waves in a Nonlinear Dielectric," Physical Review, Vol. 127, p. 1918-1939, September 15, 1962.

101. Levenson, M. D., "Feasibility of Measuring the Nonlinear Index of Refraction by Third-Order Frequency Mixing," IEEE Journal of Quantum Electronics, Vol. QE-10, p. 110-115, 2 February 1974.

102. McClung, F. J., and Weiner, D., "Measurement of Raman Scattering Cross-Sections for Use in Calculating Stimulated Raman Scattering Effect," Journal of the Optical Society of America, Vol. 54, p. 641-642, May 1964.

103. Shen, Y. R., and Bloembergen, N., "Theory of Stimulated Brillouin and Raman Scattering," Physical Review, Vol. 137, p. A1787-A1805, 15 March 1965.

104. Madhavan, D., Dheer, M. K., and Jaseja, T. S., "Nonlinear Effects Produced by Raman Maser Radiations," Applied Optics, Vol. 5, p. 1823-1828, November 1966.

105. Wang, C. C., "Nonlinear Susceptibility Constants and Self-Focusing of Optical Beams in Liquids," Physical Review, Vol. 152, p. 149-156, 2 December 1966.

106. Rado, W. G., "The Nonlinear Third Order Dielectric Susceptibility Coefficients of Gases and Optical Third Harmonic Generation," Applied Physics Letters, Vol. 11, p. 123-125, 15 August 1967.

107. Bloembergen, N., "The Stimulated Raman Effect," American Journal of Physics, Vol. 35, p. 989-1023, November 1967.

108. Maier, M., Kaiser, W., and Giordmaine, J. A., "Backward Stimulated Raman Scattering," Physical Review, Vol. 177, p. 580-599, 10 January 1969.

109. Wynne, J. J., "Optical Third-Order Mixing in GaAs, Ge, Si, and InAs," Physical Review, Vol. 178, p. 1295-1303, 15 February 1969.

110. Parsons, F. G., and Chang, R. K., "Measurement of the Nonlinear Susceptibility Dispersion by Dye Lasers," Optics Communications, Vol. 3, p. 173-176, May 1971.

111. Yablonovitch, E., Flytzanis, C., and Bloembergen, N., "Anisotropic Interference of Three-Wave and Double Two-Wave Frequency Mixing in GaAs," Physical Review Letters, Vol. 29, p. 865-868, 25 September 1972.

112. Levenson, M. D., Flytzanis, C., and Bloembergen, N., "Interference of Resonant and Nonresonant Three-Wave Mixing in Diamond," Physical Review B, Vol. 6, p. 3962-3965, 15 November 1972.

113. Hermann, J. P., Ricard, D., and Ducuing, J., "Optical Nonlinearities in Conjugated Systems: B-Carotene," Applied Physics Letters, Vol. 23, p. 178-180, 15 August 1973.

114. Levenson, M. D., and Bloembergen, N., "Dispersion of the Nonlinear Optical Susceptibilities of Organic Liquids and Solutions," The Journal of Chemical Physics, Vol. 60, p. 1323-1327, 15 February 1974.

115. Wynne, J. J., "A New Type of Nonlinear Spectroscopy Using Tunable Lasers," IEEE Journal of Quantum Electronics, Vol. QE-8, p. 607, 1972.

116. Wynne, J. J., "Nonlinear Optical Spectroscopy of $X^{(3)}$ in $LiNbO_3$," Physical Review Letters, Vol. 29, p. 650-653, 4 September 1972.

117. Begley, R. F., Harvey, A. B., Byer, R. L., and Hudson, B. S., "Raman Spectroscopy with Intense, Coherent Anti-Stokes Beams," The Journal of Chemical Physics, Vol. 61, p. 2466-2467, 15 September 1974.

118. Begley, R. F., Harvey, A. B., and Byer, R. L., "Coherent Anti-Stokes Raman Spectroscopy," Applied Physics Letters, Vol. 25, p. 387-390, 1 October 1974.

119. Itzkan, J., and Leonard, D. A., "Observation of Coherent Anti-Stokes Raman Scattering from Liquid Water," Applied Physics Letters, Vol. 26, p. 106-108, 1 February 1975.

120. Moya, F., Druet, S. A. J., and Taran, J. P. E., "Gas Spectroscopy and Temperature Measurement by Coherent Raman Anti-Stokes Scattering," Optics Communications, Vol. 13, p. 169-174, February 1975.

RECENT ISSUE BIBLIOGRAPHY

1. Weysenfeld, C. H., "Small Dye Laser in a Semi-unstable Resonator Pumped by an Argon-Jet Guided Spark," Applied Optics, Vol. 13, p. 2816-2822, December, 1974.

2. Lin, C. L., "Near-Infrared Dye Laser Emission from Ultraviolet Nitrogen-Laser-Pumped Dye Solutions," IEEE Journal of Quantum Electronics, Vol. QE-11, p. 61, January 1975.

3. Teschke, O. T., and Diennes, A., "Influence of Excited Singlet Absorption on Output Power of cw Dye Lasers," Applied Physics Letters, Vol. 26, p. 13-15, January 1975.

4. Drake, J. M., and Morse, R. I., "Influence of Chemical Impurities on the Performance of a Flashlamp-Pumped Dye Laser," Optics Communications, Vol. 13, p. 109-113, February 1975.

5. Leheny, R. F., and Shah, J., "Amplification and Excited State Absorption in Longitudinally Pumped Laser Dyes," IEEE Journal of Quantum Electronics, Vol. QE-11, p. 70-74, February 1975.

6. Smith, P. W., Liao, P. F., Shank, C. V., Lin, C., and Maloney, P. J., "The POPOP Dye Vapor Laser," IEEE Journal of Quantum Electronics, Vol. QE-11, p. 84-89, February 1975.

7. Teschke, O., Diennes, A., and Holtom, G., "Measurement of Triplet Lifetime in a Jet Stream cw Dye Laser," Optics Communications, Vol. 13, p. 318-320, March 1975.

8. Jain, K., Wozniak, W. T., and Klein, M. V., "Diffraction Grating Use to Reject Fluorescence from a Tunable Dye Laser," Applied Optics, Vol. 14, p. 811-812, April 1975.

9. Brand, H., Lange, W., Luther, J., Nottbeck, B., and Schroder, H. W., "Level-Crossing under Nearly Monochromatic Excitation by a Narrow-Band cw Dye Laser," Optics Communications, Vol. 13, p. 286-288, March 1975.

10. Maeda, M., Ishitsuka, F., and Miyazoe, Y., "Dye-Laser Amplified, Atomic Absorption Flame Spectroscopy," Optics Communications, Vol. 13, p. 314-317, March 1975.

11. Regnier, P. R., Moya, F., and Taran, J. P. E., "Gas Concentration Measurement by Coherent Raman Anti-Stokes Scattering," American Institute of Aeronautics and Astrophysics Journal, Vol. 12, p. 826-831, June 1974.

INITIAL DISTRIBUTION LIST

		No. Copies
1.	Defense Documentation Center Cameron Station Alexandria, Virginia 22314	2
2.	Library, Code 0212 Naval Postgraduate School Monterey, California 93940	2
3.	Chairman, Department of Physics and Chemistry, Code 61 Naval Postgraduate School Monterey, California 93940	1
4.	Professor William M. Tolles, Code 61 Department of Physics and Chemistry Naval Postgraduate School Monterey, California 93940	1
5.	LT. R. W. Gilbert 1155 Monarch Lane #2J Pacific Grove, California 93950	1

160974

Thesis
G4233 Gilbert
c.1 Coherent anti-Stokes Raman spectroscopy using tunable dye lasers pumped by an ultraviolet nitrogen laser.